The Effect of Surface Metal Oxide Species on Titania for the ODH of Propane: Comparison of Vanadium Oxide and Chromium Oxide Phase.

A Thesis submitted in Partial Fulfilment of the Requirements

for the Degree of

MASTER OF TECHNOLOGY

by

YETUKURI LAXMANA RAO

to the

Department of Chemical Engineering

INDIAN INSTITUTE OF TECHNOLOGY, KANPUR

December, 2002

CERTIFICATE

It is certified that the work contained in the thesis entitled **The Effect of Surface Metal Oxide Species on Titania for the ODH of Propane: Comparison of the Vanadium Oxide and Chromium Oxide Phase** by **Y. Laxmana Rao** has been carried out under my supervision and this work has not been submitted elsewhere for a degree.

Goutam Deo
Dr. Goutam Deo

Associate Professor

Department of Chemical Engineering

Indian Institute of Technology Kanpur

20th December 2002.

Acknowledgements

I am happy to express my deep gratitude towards my thesis supervisor **Dr. Goutam Deo** for his proper guidance, co-operation and encouragement. My special thanks for his patience and and kind of etiquettes I learned through out my stay with him.

I am equally thankful to faculty members Dr. Kunzru, Dr. P.K. Bhattacharya, Dr. R.P. Chabra and Dr. Kalyanmoy Deb for the help and guidance rendered by them.

My special thanks to senior lab mate Sravan for initial stages of my thesis and his valuable advises during his stay with me. I am very much thankful to Dr. Maymol Cherian for her help in the experimental work, literature study and cooperation in the lab almost through out my thesis work. I am thankful to Rohit, Mahendra and Suresh Gupta for valuable cooperation in the lab. Special thanks to my senior and lab mate Mallesh for his advises in my course and lab work. Finally, I am very much grateful to my lab mate Kamala for his help in the programming and spending the memorable lab-days with me. I thank to my junior labmates Rudrapratap and Priyanka for co-operation in the lab. I have to express my thanks to myfriend Siva Ganesh for helping me in handling TPR apparatus.

I wish to express my thanks to all my friends Sivakumar, Saurav, Narasi, Vamsi, Srinivas, Pavan, Ravi, Kishore, Asit, Rajeev, Jyoti, Negi, Neeraj and debasis

Finally, I would like to thank all my family members for their love, help and encouragement

Laxman Rao

ABSTRACT

Supported vanadium and chromium oxide on TiO_2 support were considered to understand the effect of surface metal oxide loading and type of metal oxide species on the propane ODH reaction. It was observed that for the sub-monolayer and monolayer catalysts, the propane activity increases with an increase in loading of surface metal oxide sites. The propene selectivity, however, followed different trends. To understand these two effects: the increase in surface metal oxide species and change of surface metal oxide species, the kinetic parameters were estimated for several models using Genetic Algorithms (GA). Using GA, a potential technique for parameter estimation in non-linear kinetic models, kinetic parameters were successfully determined for the different types of power law models. Based on the kinetic parameters the best-suited model for each catalyst is selected using statistical criteria based on F-test for simultaneous reactions. It was observed that the 3% V_2O_5/TiO_2 and 1% Cr_2O_3/TiO_2 are best explained by the PL-1 model for which CO and CO_2 are secondary products. However, for 4% V_2O_5/TiO_2 and 4% Cr_2O_3/TiO_2 catalysts, PL-4 and PL-3 models are best suited to explain the experimental data. The PL-4 model suggests that CO is produced as primary and secondary products and CO_2 is formed by the oxidation of CO. The PL-3 model considers that CO is secondary product and CO_2 is a tertiary product. Based on the kinetic parameters of these models the effect of loading and type of the metal oxide species is successfully explained. The main considerations being the nature of the pre-exponential factors and activation energies.

CONTENTS

List of Figures

List of Tables

Chapter 1

INTRODUCTION

Traditional sources for lighter alkenes are mainly dehydrogenation and cracking processes. However, these are relatively expensive processes. With the growing demand in petrochemical industries for lighter alkene feed stocks, it is imperative that new processes are developed. This is the impetus behind the search for potential alternatives to replace the existing traditional sources. Alternative processes like lighter alkane oxidative dehydrogenation, though still at the stage of infancy in terms of its commercial viability, appears to be more promising for various reasons of interest [1-2].

Oxidative dehydrogenation (ODH) of alkanes to alkenes is thermodynamically favoured due to formation of water, which is a stable product. An added advantage of ODH lies in its irreversible nature and, thereby, theoretically one can achieve complete conversion (100%) as there are no equilibrium constraints [2]. On the other hand, the endothermic nature of traditional processes, which are feasible at high temperatures (~1073 K), have to meet high energy requirements in contrast to the exothermic nature of ODH reaction, which is possible even at the temperature as low as 633 K. Furthermore, presence of oxygen removes deposited carbon on catalyst during the reaction resulting in less deactivation. However, there are certain hurdles to be surmounted before being a commercially feasible process. The activation of alkanes is more difficult than that of corresponding alkenes. Consequently, the alkene formed is more prone to degrade in the presence of oxygen to carbon oxides. Thus the problem lies in maximizing the formation of alkenes. Ideally, it requires a catalyst that would significantly accelerate the abstraction of hydrogen from the hydrocarbon molecule and hinder both the nucleophilic insertion of

oxygen into the molecule and the electrophilic attack of oxygen molecules on the C-C bonds [3].

In an attempt to find high selective catalysts, vanadium oxide (vanadia) supported catalyst is found to be a well-established catalyst for partial oxidation of hydrocarbons. It is widely used in the petrochemical and environmental industries. Existence of two-dimensional active species of vanadia below monolayer coverage is primarily responsible for the wide variety of applications. These applications include the ODH of propane, which is proposed to be activated by bridge V-O-V bridging bonds [4]. The catalytic activity of these oxides depends on their surface structure, character of chemical bond and the coordination unsaturation of the surface atom. The nature of the vanadium oxide species in supported vanadium oxide catalysts are known to depend on the loading and the support. Various characterization techniques have been applied to study the supported vanadium oxide phases on different metal oxides, which include, Raman spectroscopy, solid-state ^{51}V NMR spectroscopy, UV-vis DRS, and EPR studies. Detailed discussion on these spectroscopic studies is available in the literature [4-7,29].

Several recent studies are reported on ODH of isobutane and butane using chromium oxide (chromia) supported catalysts [8-11]. Similar to the supported vanadium oxide catalysts, special catalytic properties of chromium oxide species are also observed due to the interaction between the support and the chromium oxide species. Furthermore, similar to supported vanadium oxide catalysts, molecularly dispersed chromia species are more active for the ODH of propane to propene as compared to bulk Cr_2O_3 [36]. Complete understanding of structure-activity relationships requires information from

spectroscopic techniques, such as Raman, XRD, XPS, EPR and TPR along with reaction studies [32-33].

The effect of the type of the surface metal oxide phase (vanadium or chromium oxide) and the effect of the surface metal oxide loading are the factors that are required for the understanding of the ODH reaction on the metal oxide species.

Previous reaction studies using supported metal oxide catalysts are performed fulfilling various objectives, but few studies are devoted to understand the kinetic behavior and mechanism of ODH of Propane. To better understand the effect of loading and surface metal oxide species, kinetic modeling can be done. Different models include both power law typ and mechanistic models. Mechanistic models, such as Mars-van-Krevelend type redox mechanism [12,13], Rideal type mechanism [14] and mechanism involving pseudo-first-order approximation [15,16], have been proposed in order to explain kinetic behavior of ODH reaction. Detailed modeling of the ODH reaction, without pseudo-first-order approximation, contains highly non-linear functions containing local minima. Traditional methods require good initial guess in order to get global optima solutions. Genetic Algorithms (GA) provides a potential alternative to achieve global minima even when the range to be considered for parameters is extremely wide and local minima exists in the parameter space [41]. Performance of GA works on the principle of natural evolution. It also depends on parameters like crossover and mutation probabilities.

In the present study, kinetic parameters are estimated for a series of titania supported vanadium oxide catalysts and a chromium oxide on titania catalyst using rate expressions derived based on the Power Law (PL) type models. Kinetic parameters are

determined simultaneously solving non-linear mass balance equations and integrating the rate equations over entire mass using fourth order Runga-Kutta algorithm. These estimated parameters for different PL models are based on the minimization of multiple objective functions for simultaneous reactions. Parameters estimated in this way will reveal some mechanism involved in each catalyst.

1.1 Thesis objective

The present study addresses the catalytic activity of two important catalysts, namely, vanadium oxide and chromium oxide on titania support. As mentioned above two factors considered are the nature of the surface metal oxide phase and loading of the metal oxide phase. For both the catalysts, the surface metal oxide species is considered since these species form the active phase for several oxidation reactions. Several loadings of vanadium oxide are synthesized on the titanium oxide support. Chromium oxide supported on titania catalysts are considered to determine the effect of type of the metal oxide phase. The reaction parameters are obtained over the titania supported vanadium and chromium oxide catalysts using Genetic Algorithm (GA). Models are discriminated using statistical F-test criterion for simultaneous reactions [48]. Based on the results, the governing factors controlling the pathways of ODH reaction will be achieved.

2 Thesis organization

is thesis contains 5 chapters. In Chapter 2, a brief review of the literature related to the sent study is presented. In Chapter 3, details regarding preparation of the catalyst, perimental set up and the calculations are given. Brief discussion on modeling using

GA is also reported. The results obtained from the reaction studies of supported vanadia and chromia catalysts on the ODH of propane are presented and discussed in Chapter 4. In Chapter 5, conclusions and recommendations for future study are provided.

Chapter 2

LITERATURE REVIEW

Conversion of lighter alkanes to their corresponding valuable alkenes is an important process due to the increasing interest in the direct use of alkenes as potential feedstocks Alkenes find a variety of applications in the petrochemical industries. Studies in the past have primarily primarily dealt with using cobalt, nickel and antimony - molybdates based catalysts for oxidative dehydrogenation (ODH) of butane to butadiene [17-19]. Other catalysts, such as, noble metals and metal oxides are successfully tried for several dehydrogenation/oxidative dehydrogenation reactions. Metal oxides, such as, MnO_2, V_2O_5, Co_3O_4, CuO, Cr_2O_3, MoO_3, TiO_2 and ZrO_2 as bulk, as binary or in multiple composition are commonly employed for the oxidation of hydrocarbons [20-21]. Several attempts have been made to raise the yield of alkenes for ODH reaction. However, the yield of alkenes is not up to commercial exploitation. In these studies, chromium and vanadium oxide catalysts are showing promising activity. Brief summary regarding structure and activity of vanadium oxide (vanadia) and chromium oxide (chromia) catalysts based literature review is presented along with an account on modeling of ODH.

2. 1 Vanadium oxide based catalysis

Vanadia based catalysts have been extensively studied to determine their applicability in the ODH of propane reaction. Knowledge on structure-reactivity properties is essential for improving the performance of the catalyst and obtaining the fundamental information.

Deo and Wachs [7] have explained the molecular structures of the two dimensional vanadium oxides over layers on different oxide supports including titania

under ambient conditions using Raman spectroscopy. They have found that the surface vanadium oxide molecular structure depends on the net pH at point of zero charge of oxide surface. Furthermore, they observed that a strong influence of the oxide support, which was due to the difference in the V-O-support bond strength of the dehydrated surface vanadia species.

Wachs and Deo [23] have proposed several fundamental ideas regarding the structure and reactivity of vanadium oxide species on the oxide supports. Ideas regarding vanadia species include information regarding monolayer surface coverage, stability of monolayer, oxidation state, molecular structure, acidity and reactivity. They have also described physico-chemical characteristics of vanadia catalyst compared to other oxide catalysts.

Information regarding the structure of vanadia species, which decide the activity of ODH on titania support, is very essential. Grzybowska-Swierkkosz [24] has studied the distribution of various vanadia species within the monolayer coverage. Various types of species include: isolated monomers of VO_x of oxo or hydroxo type, polymeric species, V_2O_5 amorphous and crystalline forms. Types of vanadia species and their distribution depend on the morphology (rutile or anatase) of the titania support.

Bell *et al* [25] have concluded that the structure of vanadia dispersed on zirconia is strongly dependent on the surface density and calcinations temperature. It was also concluded from the analysis of catalytic and spectroscopic data that polyvanadates species, which are highly dispersed on zirconia, are responsible for the ODH of propane

Pietrzyk and Genser [26] studied the propane ODH reaction using approximately five theoretical monolayers of V_2O_5 on titania (anatase) support under

transient conditions. Regarding the prospective application of V_2O_5/TiO_2 catalyst for ODH of propane reaction in a circulatory bed reactor, these catalysts, besides requiring relatively low temperatures, have the advantage of good stability under the conditions of repeated oxidation-reduction steps.

Gao *et al.* [27] have studied the reactivity properties of the surface vanadium species by comparing the structure of the surface vanadium oxide species with their corresponding reactivity and selectivity information. In their study it was found that the V=O bond does not influence the reactivity properties of the surface vanadia species during hydrocarbon oxidation reactions. The bridging V-O-V bond, however, influences some reactions, and the V-O-support bond are found to be the most critical bond influencing the reactivity properties.

Reddy [28] characterized the V_2O_5 supported on TiO_2 catalyst. Based on Raman spectroscopy, it is observed that monolayer coverage occurs at $4\%V_2O_5/TiO_2$. During the propane ODH reaction, the activity of propane increases up to monolayer coverage and then decreases.

Banares and Cortez [29] have applied an advanced *in situ* Raman spectroscopic online measurement analysis to study the activity and structure of vanadium oxide during propane ODH reaction. This approach is considered to be a reliable since the structure-activity relationship determined during the reaction. This report concludes that surface polymeric vanadium oxide species are more reducible than isolated surface polymeric species.

2. 2 Chromium oxide based catalysis

Chromia based catalysis finds varieties of applications. Of these supported chromium oxide catalysts have been employed in several chemical reactions due to the simultaneous existence of various oxidation states. It is observed that the surface chromia species are the centers for catalytic activity. A brief summary of literature review on reactivity of chromium oxide catalyst is reported below.

Hardcastle and Wachs [30] studied the interaction of chromia with TiO_2, Al_2O_3, and SiO_2 under ambient conditions for loadings ranging between 0.5 to 5wt % of Cr_2O_3. They concluded that surface chromium oxide is present as monomers and dimers on alumina, as monomers and possibly dimers on titania, and as monomers and polymers on silica. Crystals of Cr_2O_3 appear in addition to the surface chromia species above monolayer loadings. The differences in distribution of various surface species as well as the formation of crystals occur due to the varying surface –support interaction. Based on the Raman spectroscopy.

Vuurman *et al.* [31] studied the different structures of chromia on alumina support. Based on the Raman spectroscopy, they reported that after impregnation and drying under vacuum at room temperature, chromium oxide is present as chromate for 1%Cr/Al_2O_3, as dichromate between 5 and 15% Cr/Al_2O_3, as trichromate for 20% Cr/Al_2O_3 and as crystalline CrO_3 and trichromate at 30% Cr/Al_2O_3.

Sohn *et al* [32] observed a strong influence of chromium oxide on zirconia support. The surface area of CrO_x/ZrO_2 increased with chromia loading. The authors attributed this phenomenon to the strong interaction, which prevents the support and chromia from sintering. Upon addition of only small amounts of chromia to zirconia, both the activity and acid strength significantly increased. Furthermore, Sohn *et al.* [33]

have reported that addition of chromia transforms the ZrO_2 support from amorphous to tetragonal and monoclinic phase due to strong interaction between chromia and zirconia. It was concluded by Wachs *et al.* [34] that specific oxide support is a critical parameter in deciding the reactivity of surface metal oxide species.

Scharf *et al.* [35] reported that on the surface of supported chromia at least three oxidations states (Cr(III), Cr(V) and Cr(VI)) coexist and relative contribution of three oxidation states change with loading, calcinations treatment and storage under atmospheric conditions. It was also reported that prolonged high temperature calcinations results in the decrease of chromia related bands in the Raman and IR spectra and an increased intensity of support related vibrations. They infer solid -state reaction between chromia and the support occurs which results into the incorporation of chromium into the lattice of the oxide support (TiO_2).

Cherian [36] studied the structure-reactivity properties of supported chromium oxide catalysts for propane ODH reaction with respect to support, surface area, modifiers and loading. It was observed that monolayer catalysts are the best for ODH of propane in terms of activity and selectivity. Furthermore, the monolayer Cr_2O_3/TiO_2 was more active than the Cr_2O_3/Nb_2O_5 catalyst, which was more active than the Cr_2O_3/Al_2O_3.

2.3 Kinetic modeling

Kinetic modeling provides us fundamental understanding regarding the roles of surface metal oxides on oxide support and surface metal oxide loading. Estimation of pre-exponential factors within the monolayer coverage provides the information about the variation of intrinsic kinetics of the reaction with loading. Furthermore, estimation of

activation energy will enable to predict kinetics route of a particular reaction parameters. Recently, genetic algorithm is considered an important tool for the estimation of reaction . It is considered to be robust and efficient. A summary of literature survey on ODH and parameter estimation by genetic algorithm is given below.

Parameter estimation using traditional methods, such as, Levenberg-Marquardt's methods dependent strongly on initial guess values. Different initial guess values may give rise to different solutions and are explained in the ref. [37]. On the other hand, objective functions based on non-linear models are common features in most recent parameter estimation problems. These nonlinear models using experimental data, generally contain more than one minimum for which tedious algorithms are required [38], These algorithms are sometimes susceptible to non-global optima. Thus, there is a need for development of efficient algorithms to replace the traditional methods. One such class of algorithms known as Genetic Algorithms (GA) shows promising results in terms of its accuracy and efficiency. Theoretical foundations of genetic algorithms depend on binary string representation of the solutions and the notion of schemata, template allowing the exploration of similarities among the chromosomes. This schemata representation has led to development of the schemata theorem [39].

In an attempt to find initial estimates of rate constants for non-linear chemical kinetics, Wolf *et al.* [40] have exploited GA techniques without a priori assumptions of rate determining step in order to apply for the wide range of partial pressures of reactants and temperatures. Elliot *et al* [41] have used the inversion procedure of genetic algorithm to estimate rate parameters corresponding to product species measurement data from

combustion of fuel experiments. This study suggests that its wide application to other chemical kinetics and optimization of other higher order kinetics is possible.

Moros *et al.* [42] have estimated the kinetic parameters for the dehydrodimerization of methane by using genetic algorithm. It is observed that the application of genetic algorithm to generate a good initial point for the non-linear local convergence method requires less computing time and increase the reliability of the parameters

Polifke *et al.* [43] have employed genetic algorithm to investigate the kinetic parameters of simplified reaction mechanism for methane combustion. It is also determined that using genetic algorithm requires minimum human effort and little insight into the details of chemical mechanism to generate reliable kinetic parameter.

Based on the above review it is clear that GA has not been applied to ODH reaction. Recently, Sulay has used GA to analyze the effect of support monolayer vanadia on titania and alumina and obtained promising results. However, the objective function used in that work is not amendable for multi-response systems. In this study it is observed that power law models better explain the data.

2.3.1 Kinetic studies involving ODH

Few kinetic studies involving the ODH of propane over metal oxide based catalysts exist. A brief review of these studies is given below.

Andersson [14] studied the partial pressure dependencies of propane oxidation. The corresponding rate expression, which is in accordance with Rideal type rate expression for various concentrations of vanadium on amorphous $AlPO_4$, is adequate to

explain the partial pressure dependencies of both oxygen and propane. A first order dependency of propane for the ODH reaction is proposed.

Chen *et al.* [16] performed kinetic isotopic studies for the ODH of propane on 10% V_2O_5/ZrO_2 catalyst. The activation of methylene C-H bond is found to be the kinetically relevant step for the ODH of propane, while for secondary combustion allylic C-H bond in propene is rate-controlling step. Furthermore, Chen *et al.* [44] proposed that the breakings of C-H bond, dissociative adsorption of oxygen are irreversible steps.

Creaser and Andersson [12] have undertaken a detailed kinetic investigation of ODH on V-Mg-O catalyst. Various rate expressions are derived in order to fit the data based on Power Law type models as well as mechanistic models, such as Langmuir-Hinshelwood and Mars-Van-Krevelen models. In all the models, they have considered carbon oxides as secondary products. However, in a later study Creaser *et al.* [13] have concluded that the reaction data is best explained by considering carbon oxides as primary and secondary combustion product. Furthermore, they have proposed involvement of lattice oxygen in the ODH reactions.

2.4 Summary

From the above review, it is clear that supported vanadium oxide and chromium oxide show the promising catalysts for the propane ODH reaction. The literature review of the characterization and reaction studies for the supported vanadium and chromium oxide catalysts reveal that surface metal oxide species form a unique phase, which is physically

and chemically different from the bulk phase. Oxide support and metal oxide loading are critical parameters in deciding the nature of the metal oxide species and its reactivity. To understand the effect of surface metal oxide phase, Cr_2O_3/TiO_2 and V_2O_5/TiO_2 are considered for propane ODH reaction. Furthermore, to understand the effect of loading, several loadings of V_2O_5/TiO_2 are also studied. The effect of metal oxide phase and metal oxide loading is studied with the help of observing the changes, if any, in the kinetic parameters. The kinetic parameters are estimated using GA.

CHAPTER 3

EXPERIMENTAL DETAILS

3.1 Catalyst Preparation

Catalyst samples used in the present study were prepared by the incipient wetness impregnation method. This method is known for its simplicity and viability for making low amounts of metal oxide catalysts. Two types of catalysts were prepared: a series of supported vanadium oxide (vanadia) catalysts and supported chromium oxide (chromia) catalysts. Titania is used as the support. The precursors used for supported vanadia and chromia catalysts were ammonium metavanadate (NH_4VO_3) and chromium nitrate nanohydrate ($Cr(NO_3)_3 .9H_2O$, Aldrich, 99.98% purity), respectively. Prior to preparing supported vanadia catalyst the support, titania (Degussa, P-25, $55m^2/g$), was initially pretreated with incipient volumes of known concentration of oxalic acid solution. The support was then dried at room temperature in a desiccator followed by drying at 383 K for 8 h. The support was finally calcined at 723 K for another 8 h. Prior to making the supported chromia catalyst the support was pretreated with incipient volumes of water. The heating treatment similar to the above was then followed.

For the supported vanadia series, the incipient wetness impregnation method of the above-pretreated support was carried out with a solution of vanadium oxalate precursor. The vanadium oxalate solution was prepared by adding known amounts of ammonium meta vanadate with stoichiometric amount of oxalic acid to distilled water. Stirring of this mixture was done until a homogeneous solution was formed. The deep blue solution formed by the above method was further diluted with double distilled water such that the total volume corresponds to the incipient wetness impregnation volume of

the support. The pretreated support was then taken in a crucible and the precursor solution was added drop wise and mixed. The paste was then heat treated as described for the pretreatment of the support. By this method 1, 3 and 4% V_2O_5 loadings on titania support are prepared. Additional details can be found in elsewhere [28].

For the chromia-titania catalyst, a predetermined amount of chromium nitrate nanohydrate precursor was intimately mixed with incipient wetness volume of water and subsequent heat treatment conditions for this catalyst were similar to those described for the supported vanadia catalyst. In this way, 1 and 4% Cr_2O_3 loadings on titania support were prepared. Additional details can be found in elsewhere [36]. For both catalyst x% refers to the weight percent of vanadia or chromia, in terms of V_2O_5 or Cr_2O_3, in the catalyst.

3.2 Experimental Set up

The oxidative dehydrogenation (ODH) of propane was performed in a down flow tubular quartz reactor with inlet dia 10 mm and outlet dia 5 mm. The catalyst sample amounts used in the reaction ranged from 0.03 to 0.15 g and is given in Table 3.1. Quartz powder was used as a diluent and well mixed with supported catalysts in order to prevent temperature gradients and to avoid the channeling of gas within the catalyst bed. This mixture of catalyst and quartz powder was placed on the well-seated quartz wool at the center of the 300 mm long quartz reactor. The catalyst was placed in the isothermal zone of the furnace. A schematic view representing the flow diagram of the experimental set up is shown in Fig 3.1.

The reactant mixture of propane and air at different molar ratios were used with a total flow rate of 50 ml/min. Propane to oxygen molar ratios used for both series of supported vanadia and chromia samples ranged from 1:1 to 4:1 and the temperature window of operation was from 633K to 733K. The flow rate of propane and air was controlled by separate mass flow controllers (**Bronkhost Hi-Tech, Model F-201D and Model F-201C**). A Chromel-Alumel thermocouple was inserted from the top of the reactor as a sensor in a feedback control loop, central to which was a PID controller (**Fuji PXZ-4)** capable of controlling the reactor temperature within $1\ ^{0}$ C range of accuracy to the set point.

Analysis of product gases was achieved using an on-line gas chromatography (**NUCON, MODEL-5765**), which was equipped with an activated alumina column for separation of propane, propene, CO and CO_2. The GC oven temperature was maintained at 327 K and the analysis was performed with the help of a flame ionization detector (FID). Carbon oxides, CO and CO_2, were converted to methane by a methanizer in order to be detected by the FID. Main components of the reactor outlet were propane, propene, CO and CO_2. No extra products were observed in case of the vanadia series of samples. However, in case of chromia other peaks were observed at high temperatures, which could be attributed to oxygenated peaks. Data for each experimental condition was collected thrice. Blank runs revealed that there was no propane conversion in the experimental region considered suggesting that homogeneous reaction did not take place.

3.3 Reactivity Calculations

Analyzed products of the reaction were propene, carbon monoxide, carbon dioxide and unconverted propane. Each of these components gave separate areas in the

chromatograph. The calculations of conversion, activity, selectivity and yield per gm catalyst were based on mole fractions. The area of each component is converted to mole fraction based on the response factor given in Table 3.2.

3.3.1 Conversion

Conversion for this reaction can be calculated by using following formulae,

$$\text{Conversion, \%} = \frac{\text{Moles of Propane converted}}{\text{Moles of Propane in}} \times 100$$

$$= \frac{\text{Moles of Propane in - Moles of Propane out}}{\text{Moles of Propane in}} \times 100 \qquad (3.1)$$

3.3.2 Selectivity

Selectivity for the reactions leading to formation of propene was calculated as follows:

$$\text{Propene selectivity, \%} = \frac{\text{Moles of Propene formed}}{\text{Moles of Propane converted}} \times 100 \qquad (3.2)$$

3.3.3 Yield

The amount of propene formed was represented by yield, which was calculated as follows:

$$\text{Propene yield, \%} = \frac{\text{Moles of Propene formed}}{\text{Moles of Propane in}} \times 100 \qquad (3.3)$$

3.3.4 Carbon Balance

Carbon balance represents the accuracy of measurements and provides an indicator as to whether carbon is deposited on the catalyst. Carbon balance calculations are performed based on the formula given below.

$$\text{Carbon balance, \%} = \frac{\text{Moles of Carbon out}}{\text{Moles of Carbon in}} \times 100 \qquad (3.4)$$

3.4 Kinetic Modeling of ODH

Improvement of kinetic modeling for ODH reaction in the absence of well-accepted mechanism is still a challenging task. It initially involves, modeling of this complex reaction followed by estimation of kinetic parameters. Subsequently insight for pathways of different products can be obtained.

3.4.1 Parameter Estimation

Earlier attempts to estimate kinetic parameters include linearisation of the rate equation so that ordinary least square methods can be applied. However, it is always not possible to linearize rate expression of heterogeneous catalytic reactions and often the estimation of rate parameters is achieved by nonlinear regression methods. Consequently, practical problems due to non-linearity of the models and limitations of traditional optimization methods are usually encountered. The objective function based on nonlinear model for the kinetic study of experimental data usually contains more than one optimum and there by traditional methods are prone to non-global optima solutions.

The present study involving the estimation of parameters from propane ODH reaction makes use of an evolutionary search algorithms called Genetic Algorithm (GA). This is a class of algorithm that is mainly dictated by Darwinian principle of survival of the fittest [41]. The successful identification of reasonable parameters gives insight about catalyst dependent kinetics of the reaction. Procedure for modeling of ODH reaction, outlines of GA technique and different reaction schemes for Power Law type models is presented here.

3.4.1.1 Modeling of reaction

Kinetic analysis of the ODH reaction is performed using the integral method. Reaction rate equations with coefficients that have Arrhenius dependence on temperature require nonlinear procedure to obtain rate constants. Non-linear regression analysis has the following advantages over conventional linear regression approach:

- To find r_A, traditional methods require plots of X_A vs. W/F_{AO}. Drawing the tangent at various points gives the rate. This is somewhat subjective in nature and usually not reproducible.
- During linearization, taking reciprocals and cross-multiplication in mechanistic models distort the error structure because the r_A quantity is in the denominator. The error in r_A is meaningful when r_A is small.
- Conventional methods are mostly applicable for single reaction. For complex reaction systems, however, each of the rates is not known. Therefore in these cases the integral approach is useful.

Other advantages in detail are described elsewhere [46]

The following assumptions are made for better implementation of the reaction

- The reaction is operated under steady state isothermal conditions.
- Total numbers of moles of gases remain constant.
- Gas phase reactions are negligible.
- Catalyst activity is not affected due to deactivation.

These assumptions are justified since propane conversions are maintained less than 10%, several runs are taken at each experimental condition and no reaction occurs in an empty reactor

MATERIAL BALANCE: Material balance calculations based on the above assumptions for each component, i, and a particular reaction network can be written as

$$V_0 x_i|_W - V_0 x_i|_{W+dW} - \sum_j n_{ij} r_j dW = 0 \qquad i = 1.....p \qquad (3.1)$$

Where,

V_0 = volumetric flow rate of the feed

x_i = mole fraction of the i^{th} component

n_{ij} = stoichiometric coefficient of the i^{th} component for the j^{th} reaction

r_j = rate of j^{th} reaction in terms of volume per unit mass of catalyst per unit time and is a function of $\boldsymbol{K}_j$ and x_i

$\boldsymbol{K}_j$ = kinetic parameters for the j^{th} reaction

W = weight of the catalyst.

p = number of components

Simplification of equation 3.1 using above assumptions gives rise to

$$\frac{dx_i}{dW} = \sum_j n_{ij} r_j \Big/ V_0 \qquad i = 1.....p \qquad (3.2)$$

The set of ordinary differential equations represented by equation 3.2 can be solved to obtain the output mole fraction of each component based on the input value of mole fraction, x_{io} and knowledge of r_j. The initial mole fraction is changed during integration over the entire mass using Runga-Kutta fourth order technique. The specific rate of reaction, r_j, is dependent on values of kinetic parameter K_j, and some or all mole fractions, x_i. For a particular set of input parameters and the functional dependency, $r_j = f_j(x_i, \boldsymbol{K}_j)$, the integration of the above equation will give the output mole fraction. The predicted the output mole fraction obtained this way can then be compared with actual

output mole fraction. Minimization of the difference between the actual and predicted mole fraction forms the basis for changing the parameter values, K_j, by GA. For multi-response systems, the objective function is suitably modified and discussed later in section 3.4.2.3.

3.4.2 The concept of Genetic Algorithm (GA)

Genetic algorithms are different from most classical optimization methods. Principles of GA techniques are based on natural genetic inheritance and selection of evolution process. These are multidirectional search and optimization procedures that combine survival of the fittest among a set of string structures with a structured yet randomized information. The string structures are modified based on experience. New sets of artificial strings are created in every generation using bits and pieces of the fittest of the old artificial strings. These GA's are known for striking the balance between exploration and exploitation of given search space to estimate parameters [41].

3.4.2.1 Optimal problem formulation using GA

Problem formulation procedure is necessary to create a mathematical model for the present optimal design problem of parameter estimation. GA requires choosing required variables, constraints, objective function and variable bounds. A detailed optimal problem procedure for general case is described in [45,47].

3.4.3.2 Working principle

Genetic algorithms possess the advantage of not using an initial estimate of parameters for its operation. Some of the features of GA used in the present study are given below.

CODING: The GA variables are coded (binary or real) from lower to upper bound on the variable to form a string. The theoretical foundations of genetic algorithm depend on binary string representation of solutions and on the notion of schemata and templates allowing exploration of similarities among the chromosomes.

ASSIGNING FITNESS TO SOLUTION: The objective function evaluated at certain values of variables is transformed to non-negative values based on the fitness function. The fitness or objective function considered is discussed in section 3.4.2.3. The GA searches for solutions that minimize the fitness function.

REPRODUCTION OPERATION: The primary objective of the reproduction operator is to emphasis good solution and eliminates bad solution while keeping the population size constant. Using this operator multiple copies of good solution are made and bad solution are eliminated based on a probabilistic approach.

CROSSOVER OPERATOR: Crossover is the mating process that allows information exchange from one generation to the next. In crossover, two randomly chosen strings exchange their sub-strings to create two new strings. The number of crossover operations is controlled by the crossover probability, Pc, which represents the probability that a particular pair of chromosomes is selected for crossover. If the crossover is too high then highly fit individuals are discarded faster than selection can produce the improvements. On the other hand, if it is too low, selection may stop for lack of exploration. Usually Pc value lies between 0.5 and 1.0 [41].

MUTATION OPERATOR: The mutation operator changes a 1 to a 0 and vice a versa in a binary string to create a new string, which hopefully have better fitness value. The mutation operation is controlled by the mutation probability, P_m. The optimum balance between convergence and divergence is maintained by a high P_m and low Pc. The values of Pm and Pc used in the present study are 0.006 and 0.9 respectively.

3.4.2.3 Objective function

To obtain the optimized kinetic parameters, the choice of the objective function is critical. Various objective functions like minimization of sum of the squares (SOS) of deviations between outlet and inlet concentrations are extensively used in the optimization problems. However, in the present case, there are several simultaneous inlets and outlet concentration values are present, i.e., the system has multiple responses. During situations dealing with multi response systems the minimization of following determinant as an objective function is shown to be better [48].

$$\det \begin{vmatrix} \Sigma (X_{i1,\,expt} - X_{i1,\,pred})^2 & \Sigma [(X_{i1,expt} - X_{i1,perd})(X_{i2,expt} - X_{i2,pred})] & \Sigma [(X_{i1,expt} - X_{i1,perd})(X_{i3,expt} - X_{i3,pred})] & \Sigma [(X_{i1,expt} - X_{i1,perd})(X_{i4,expt} - X_{i4,pred})] \\ \Sigma [(X_{i1,expt} - X_{i1,pred})(X_{i2,expt} - X_{i2,pred})] & \Sigma (X_{i2,expt} - X_{i2,perd})^2 & \Sigma [(X_{i2,expt} - X_{i2,perd})(X_{i3,expt} - X_{i3,pred})] & \Sigma [(X_{i2,expt} - X_{i2,perd})(X_{i4,expt} - X_{i4,pred})] \\ \Sigma [(X_{i1,expt} - X_{i1,pred})(X_{i3,expt} - X_{i3,pred})] & \Sigma [(X_{i2,expt} - X_{i2,perd})^2 (X_{i3,expt} - X_{i3,pred})] & \Sigma [(X_{i3,expt} - X_{i3,perd})^2 & \Sigma [(X_{i3,expt} - X_{i3,perd})(X_{i4,expt} - X_{i4,pred})] \\ \Sigma [(X_{i1,expt} - X_{i1,pred})(X_{i4,expt} - X_{i4,pred})] & \Sigma [(X_{i2,expt} - X_{i2,perd})^2 (X_{i4,expt} - X_{i4,pred})] & \Sigma [(X_{i3,expt} - X_{i3,perd})(X_{i4,expt} - X_{i4,pred})] & \Sigma [(X_{i4,expt} - X_{i4,perd})^2 \end{vmatrix}$$

The problem then can be formulated as minimization of the above determinant with respect to K_j, which will give the true estimate of kinetic parameters for a particular function dependency, $r_j = f_j(x_i, K_j)$.

3.4.3.4 Variable bounds

GA requires certain bounds to be set on each parameter. Optimized parameter values should lie within the chosen parameter limits. Ideally GA will access global minimum in the bounds of the parameters search space in spite of local minima being present in the parameter space.

3.4.4 Reaction schemes

The kinetic study of propane ODH includes various empirical and mechanistic models. These models proposed can be broadly classified as Power law type models and mechanistic models. Most of the models suggest that propene formation is a result of primary reaction. However, the formation of carbon oxides as primary or secondary reactions is still debatable. Here discussion is confined to Power Law based models and details about mechanistic models, such as Langmuir-Hinshelwood model, Rideal type model, Mars-van-Krevelen model and model involving pseudo-first-order approximations are not considered

The reaction of propane with oxygen can be presented in the form of six reactions steps, r_1 to r_6, as shown with the generalized scheme in Fig.3.2. Propene is formed by the ODH of propane (r_1), which can degrade to form CO and CO_2 by reaction r_2 and r_3,

respectively. The carbon oxides, CO and CO_2, can also be formed directly from propane by reaction r_4 and r_5, respectively. Furthermore, CO_2 can be formed by the oxidation of CO by reaction r_6. Carbon containing compounds are only shown in Fig 3.2.

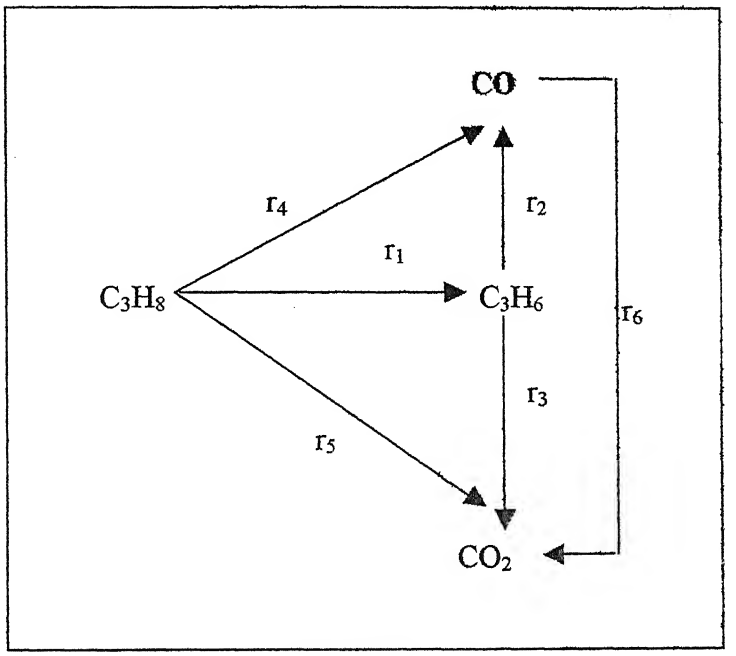

Fig 3.2 Generalized scheme for Power Law model reaction network

The stoichiometric equations corresponding to each reaction in the reaction network shown in Fig. 3.2 can be written as

$$C_3H_8 + 0.5O_2 \rightarrow C_3H_6 + H_2O \quad (3.3)$$

$$C_3H_6 + 3O_2 \rightarrow 3CO + 3H_2O \quad (3.4)$$

$$C_3H_6 + 4.5O_2 \rightarrow 3CO_2 + 3H_2O \quad (3.5)$$

$$C_3H_8 + 3.5O_2 \rightarrow 3CO + 4H_2O \quad (3.6)$$

$$C_3H_8 + 5O_2 \rightarrow 3CO_2 + 4H_2O \quad (3.7)$$

$$CO + 0.5O_2 \rightarrow CO_2 \quad (3.8)$$

3.4.5 Power law models

Several power law models were analyzed to determine the empirical reaction rates, which can further be used to develop mechanistic models. In the power law models it is assumed that the reaction rate is proportional to the partial pressure of reactant raised to a particular exponent. Based on the reaction scheme given in Fig. 3.2 the rate expression are expressed as

$$r_1 = k_1 \left(\frac{P_{C3H8}}{P^m_{C3H8}}\right)^{a1} \left(\frac{P_{O2}}{P^m_{O2}}\right)^{b1} \tag{3.9}$$

$$r_2 = k_2 \left(\frac{P_{C3H6}}{P^m_{C3H6}}\right)^{a2} \left(\frac{P_{O2}}{P^m_{O2}}\right)^{b2} \tag{3.10}$$

$$r_3 = k_3 \left(\frac{P_{C3H6}}{P^m_{C3H6}}\right)^{a3} \left(\frac{P_{O2}}{P^m_{O2}}\right)^{b3} \tag{3.11}$$

$$r_4 = k_4 \left(\frac{P_{C3H8}}{P^m_{C3H8}}\right)^{a4} \left(\frac{P_{O2}}{P^m_{O2}}\right)^{b4} \tag{3.12}$$

$$r_5 = k_5 \left(\frac{P_{C3H8}}{P^m_{C3H8}}\right)^{a5} \left(\frac{P_{O2}}{P^m_{O2}}\right)^{b5} \tag{3.13}$$

$$r_6 = k_6 \left(\frac{P_{CO}}{P^m_{CO}}\right)^{a6} \left(\frac{P_{O2}}{P^m_{O2}}\right)^{b6} \tag{3.14}$$

Where,

k_i	is the rate constant for reaction i, and
a_i and b_i	are the partial pressure exponent of the reactant for reaction i

In these reactions the partial pressures are centered around a particular mean pressure p_i^m and discussed later.

3.5.1.1 PL-1 model

The PL-1 model assumes that CO and CO_2 are secondary products and are formed from propene. Thus r_1, r_2 and r_3 are the only reactions considered since r_4, r_5 and r_6 are insignificant. This reaction model is shown in Fig 3.3.

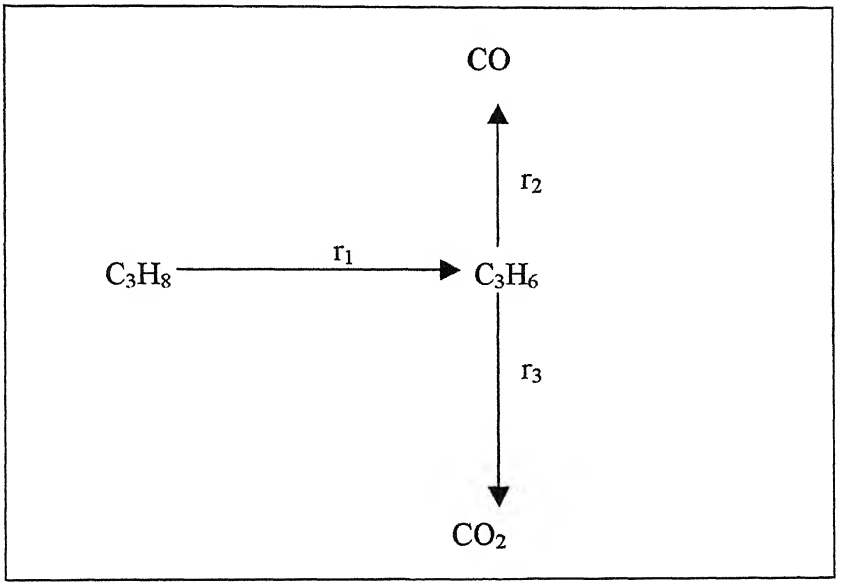

Fig 3.3 PL-1 reaction model

Based on the reaction scheme given in Fig 3.3 the rate expression are expressed as

$$r_1 = k_1 \left(\frac{P_{C3H8}}{P^m_{C3H8}}\right)^{a1} \left(\frac{P_{O2}}{P^m_{O2}}\right)^{b1} \tag{3.15}$$

$$r_2 = k_2 \left(\frac{P_{C3H6}}{P^m_{C3H6}}\right)^{a2} \left(\frac{P_{O2}}{P^m_{O2}}\right)^{b2} \tag{3.16}$$

$$r_3 = k_3 \left(\frac{P_{C3H6}}{P^m_{C3H6}}\right)^{a3} \left(\frac{P_{O2}}{P^m_{O2}}\right)^{b3} \tag{3.17}$$

Rate expression represented by r_1, r_2 and r_3 are the rates of formation of propene, carbon monoxide and carbon dioxide respectively.

3.5.1.2 PL-2 model

The PL-1 model given above is modified, considering that CO and CO_2 can be primary and /or secondary products. Propane reacts to form CO, CO_2 and C_3H_6. In this model r_6 is insignificant. The reaction scheme is shown in the Fig 3.4.

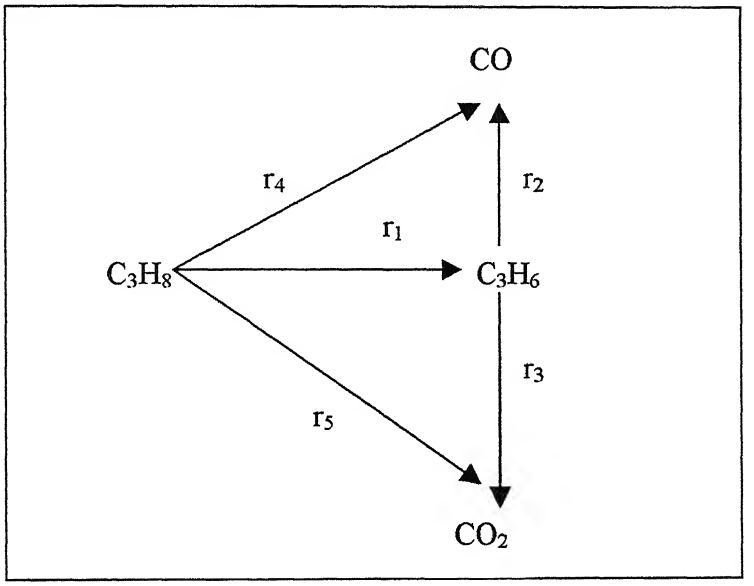

Fig 3.4 PL-2 reaction model

The rate expression are expressed as

$$r_1 = k_1 \left(\frac{P_{C3H8}}{P^m_{C3H8}}\right)^{a1} \left(\frac{P_{O2}}{P^m_{O2}}\right)^{b1} \tag{3.18}$$

$$r_2 = k_2 \left(\frac{P_{C3H6}}{P^m_{C3H6}}\right)^{a2} \left(\frac{P_{O2}}{P^m_{O2}}\right)^{b2} \tag{3.19}$$

$$r_3 = k_3 \left(\frac{P_{C3H6}}{P^m_{C3H6}}\right)^{a3} \left(\frac{P_{O2}}{P^m_{O2}}\right)^{b3} \tag{3.20}$$

$$r_4 = k_4 \left(\frac{P_{C3H8}}{P^m_{C3H8}}\right)^{a4} \left(\frac{P_{O2}}{P^m_{O2}}\right)^{b4} \tag{3.21}$$

$$r_5 = k_5 \left(\frac{P_{C3H8}}{P^m_{C3H8}}\right)^{a5} \left(\frac{P_{O2}}{P^m_{O2}}\right)^{b5} \tag{3.22}$$

3.4.5.3 PL-3 model

In this model, it is assumed that CO_2 is formed from CO only. The series reaction involved is propane giving rise to propene, which further reacts to form CO. The CO formed oxidizes to CO_2. Thus, r_1, r_2 and r_6 are the only reactions occurring and the rest are insignificant. The reaction network is given in Fig 3.5 and corresponding rate equations are shown below.

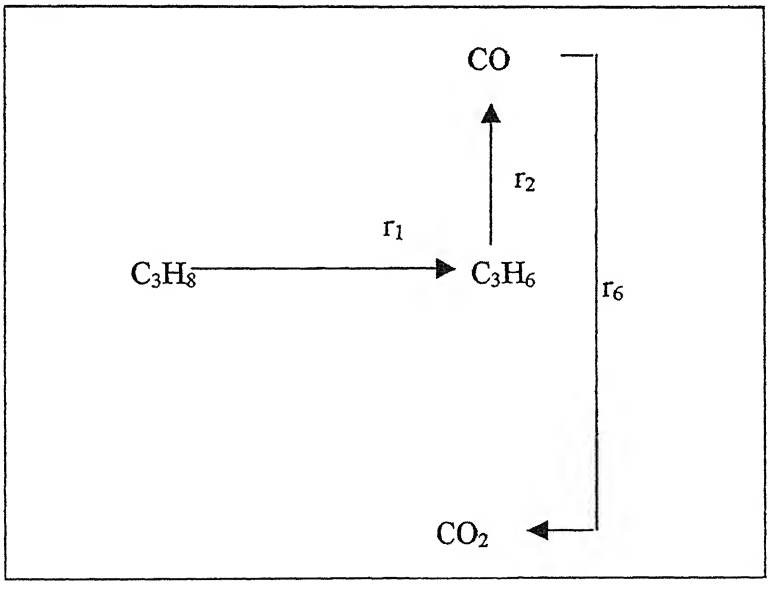

Fig 3.5 PL-3 reaction model

$$r_1 = k_1 \left(\frac{P_{C3H8}}{P^m_{C3H8}}\right)^{a1} \left(\frac{P_{O2}}{P^m_{O2}}\right)^{b1} \tag{3.23}$$

$$r_2 = k_2 (\frac{P_{C3H6}}{P_{C3H6}^m})^{a2} (\frac{P_{O2}}{P_{O2}^m})^{b2} \quad (3.24)$$

$$r_6 = k_6 (\frac{P_{CO}}{P_{CO}^m})^{a6} (\frac{P_{O2}}{P_{O2}^m})^{b6} \quad (3.25)$$

3.4.5.4 PL-4 model

The PL-3 model is further modified to consider a parallel path for CO production from propane. The reactions occurring are r_1, r_2, r_4 and r_6 and are shown in Fig 3.6. The reactions r_3 and r_5 are insignificant. The corresponding rate equations for r_1, r_2, r_4 and r_6 are given below.

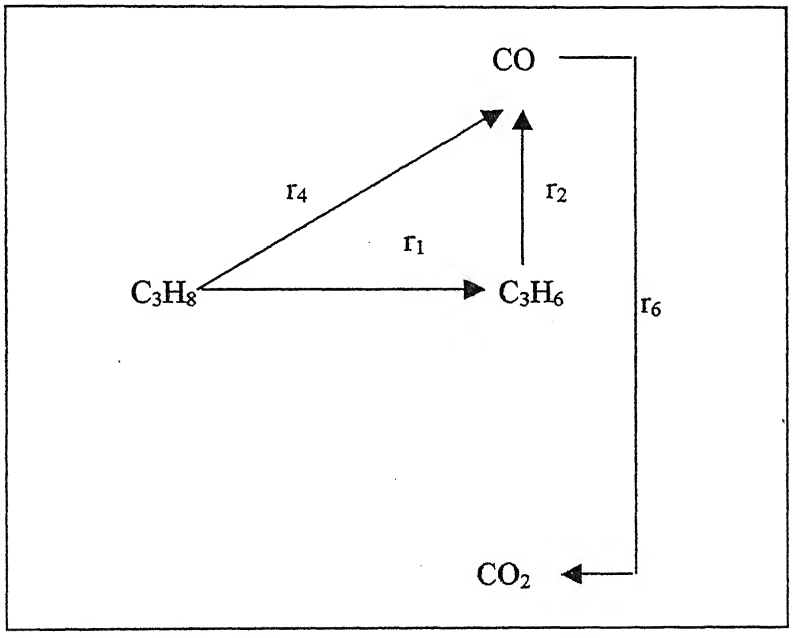

Fig 3.6 PL-4 reaction model

$$r_1 = k_1 (\frac{P_{C3H8}}{P_{C3H8}^m})^{a1} (\frac{P_{O2}}{P_{O2}^m})^{b1} \quad (3.26)$$

$$r_2 = k_2 (\frac{P_{C3H6}}{P^m_{C3H6}})^{a2} (\frac{P_{O2}}{P^m_{O2}})^{b2} \quad (3.27)$$

$$r_3 = k_3 (\frac{P_{C3H6}}{P^m_{C3H6}})^{a3} (\frac{P_{O2}}{P^m_{O2}})^{b3} \quad (3.28)$$

$$r_5 = k_5 (\frac{P_{C3H8}}{P^m_{C3H8}})^{a5} (\frac{P_{O2}}{P^m_{O2}})^{b5} \quad (3.29)$$

$$r_6 = k_6 (\frac{P_{CO}}{P^m_{CO}})^{a6} (\frac{P_{O2}}{P^m_{O2}})^{b6} \quad (3.30)$$

The number of parameters associated with the various power law models is given in Table 3.3. Various parameters for Power Law models and their ranges of search for the present discussion of ODH reaction are reported in the Table 3.4. Number of kinetic parameters depends on the type of the model selected as well as assumptions made in that proposed model.

3.6 Model selection

When replicate experiments are not available and in the absence of error analysis, F-test, a statistical criterion for simultaneous reactions, is used to select suitable model that best explains the reaction data.

$$F_c = \frac{\sum_{h=1}^{v}\sum_{k=1}^{v}\sigma^{hk}\sum_{i=1}^{n}\hat{y}_{ih}\hat{y}_{ik}/p}{\sum_{h=1}^{v}\sum_{k=1}^{v}\sigma^{hk}\sum_{i=1}^{n}(y_{ih}-\hat{y}_{ih})(y_{ik}-\hat{y}_{ik})/(nv-p)}$$

where,

y_{ih}= Experimental concentration of h^{th} response in i^{th} experiment

$\hat{y}_{ik}$ = Predicted concentration of k^{th} response in i^{th} experiment

p = Number of kinetic parameters in a model

n = Number of experiments

v=Number of responses

σ^{hk} =Elements of inverse of the (v x v) error covariance matrix.(=1)

Among the set of available models, one with highest F_c will be considered to be the best among the set of rival models [48].

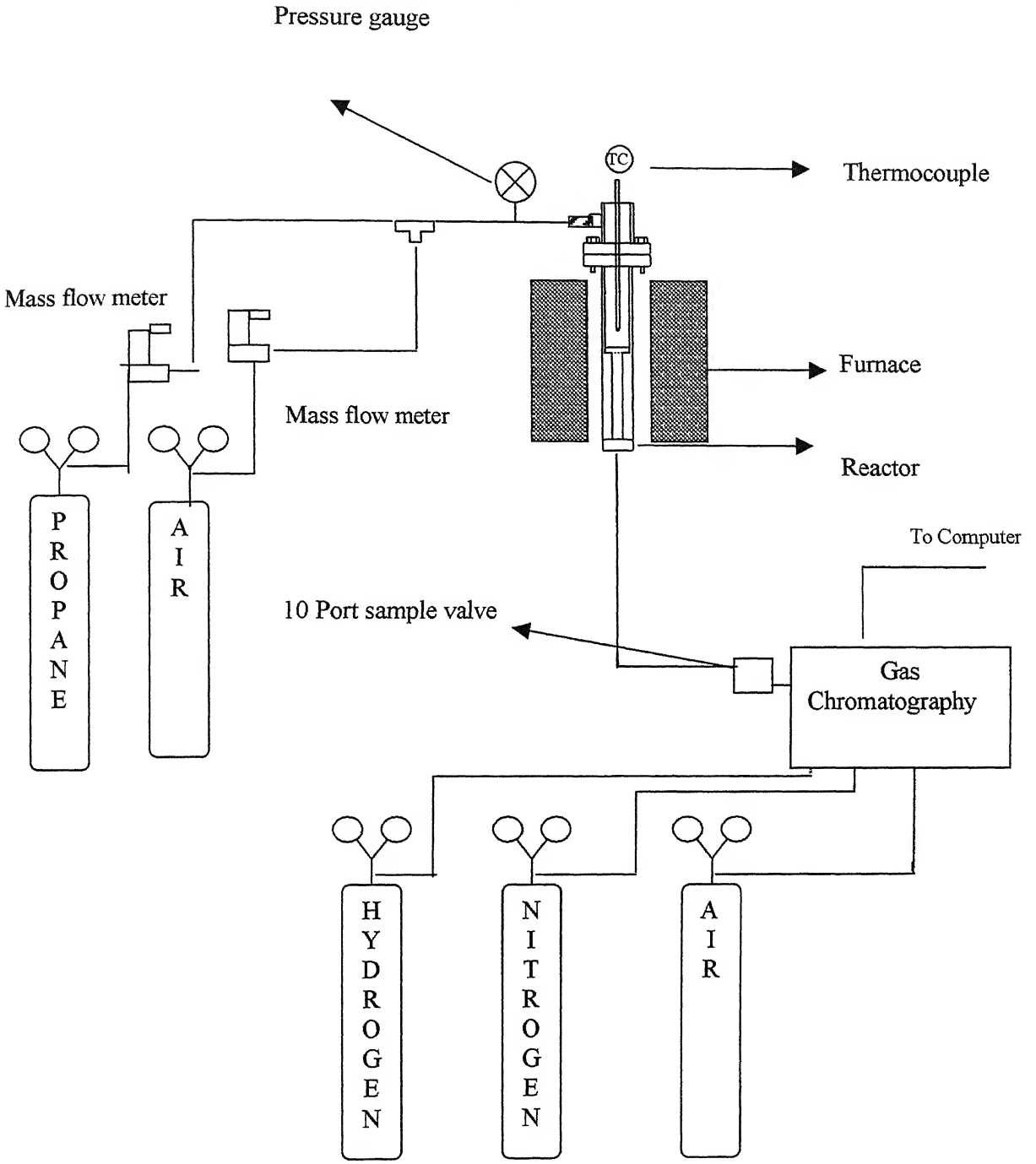

Fig 3.1 REACTOR SETUP FOR PROPANE ODH REACTION

Table 3.1: Different weights of catalyst samples used during reaction studies

Catalyst	Weight (g)
1% V_2O_5/TiO_2	0.100
3% V_2O_5/TiO_2	0.040
4% V_2O_5/TiO_2	0.030
1% Cr_2O_3/ TiO_2	0.150
4% Cr_2O_3/ TiO_2	0.050

Table 3.2: Response factor values used in carbon balance.

Component	Response Factor
Propane	0.6162
Propene	0.8744
Carbon Monoxide	1.0000
Carbon Dioxide	1.0000

Table 3.3 Different Power Law models and corresponding number of kinetic parameters

KINETIC MODEL	CONTRIBURTING RATES	NUMBER OF PARAMETERS				
		k_{io}	E_i	a_i	b_i	Total
PL-1	r_1, r_2, r_3.	3	3	3	3	12
PL-2	r_1, r_2, r_3, r_4, r_5.	5	5	5	5	20
PL-3	r_1, r_2, r_6.	3	3	3	3	12
PL-4	r_1, r_2, r_4, r_6.	4	4	4	4	16

Table 3.4 Lower and upper bounds of the kinetic parameters for Power Law models

Kinetic parameter	unit	Bounds	
		Lower	Upper
K_{i0}.	$ml\ STP\ min^{-1}\ (g\ cat)^{-1}\ atm^{-(ai+bi)}$	0.01	20
E_i.	$kJ\ mol^{-1}$	20	200
a_1, b_1.	Dimensionless	0.01	1.00

Chapter 4

RESULTS AND DISCUSSION

4.1 Characterization studies

Characterization studies provide information about the nature of active species. Combining spectroscopic studies with reaction data is very handy in order to interpret experimental and modeling results.

The surface areas of V_2O_5/TiO_2 samples for different loadings are almost constant (~ 40 m^2/g) for 1 to 4% V_2O_5 loadings. BET areas for different V_2O_5/TiO_2 loadings are reported in Table 4.1. The XRD studies does not detect separate peak corresponding V_2O_5 phase. However, from Raman spectroscopic studies obtained under ambient conditions, the presence of V_2O_5 crystals are detected for the loadings above ~ 4% V_2O_5/TiO_2 sample [28]. Thus, monolayer coverage is achieved for 4% V_2O_5/TiO_2. Similar kind of Characterization analysis for Cr_2O_3/TiO_2 samples is performed. BET areas of different Cr_2O_3/TiO_2 loadings are ranged from 40 to 60 m^2/g (pure titania). These BET areas for different Cr_2O_3/TiO_2 loadings are also reported in the Table 4.1. From Raman and other spectroscopic studies, it is observed that monolayer coverage is achieved at ~ 4% Cr_2O_3/TiO_2. *In situ* Raman and DRS characterization studies under dehydrated conditions revealed the presence of dispersed surface Cr^{6+} oxide species for the samples below monolayer loadings. Additional Cr^{5+} and δ - Cr^{3+} species were detected by EPR [36].

Below the monolayer coverage both vanadia and Chromia surface species are present in the respective catalysts. The nature of these surface metal oxide species have

been studied by various techniques and structures of the surface vanadia and Chromia have been proposed [49].

4.2 Reaction studies

Reaction studies were carried out over 1, 3 and 4% V_2O_5/TiO_2 and 1 and 4% Cr_2O_3/TiO_2 catalysts. During the reaction studies the total feed flow rate was maintained at 50 cc/min and propane to oxygen gas ratio was varied from 1:1 to 2:1 to 3:1 to 4:1. A known amount of catalyst was placed in the isothermal zone of the furnace. All the runs were taken in the temperature range of 633 to 733 K with 20 K difference between the consecutive runs. At each reaction condition data is collected thrice. Based on the inlet propane (C_3H_8) and oxygen (O_2) concentrations and outlet areas detected by GC, the input and output mole percents of C_3H_8, C_3H_6, CO and CO_2 are tabulated in the Tables 4.2 to 4.6. In these Tables the first column corresponds to reaction temperature. The second and third major columns give the input (C_3H_8 and O_2) and output (C_3H_8, C_3H_6, CO_2 and CO) mole percents. The last column gives the C-balance in terms of the ratio of carbon atoms out to carbon atoms in, C_{out}/C_{in}, and is a measure of the accuracy of analysis. The data in each Table is organized such that propane to oxygen ratio of 1:1 is the top set of data and is separated by a gap from the following ratio 2:1 data, which is followed by the 3:1 and then the 4:1 data. In each data set, corresponding to a particular propane to oxygen ratio, the data is presented in increasing reaction temperatures.

4.2.1 The effect of vanadia loading on activity and propene selectivity

Previous studies on the same catalysts have suggested that the activity during the propane ODH increases with metal oxide loading up to monolayer coverage [28]. To confirm this

objective, the activity and propene selectivity for 1, 3 and 4% V_2O_5/TiO_2, from the data given in the Tables 4.2 to 4.4 and are shown in the Figs 4.1 to 4.4. In the Figs. 4.1 to 4.4, the molar ratio of C_3H_8:O_2 changes from 1:1 to 2:1 to 3:1 to 4:1. For all these C_3H_8:O_2 ratios, the activity increases with loading for the temperature range used in the present study. The catalytic activity also increases with increase in temperature, which is expected. Furthermore, for a particular catalyst, the activity appears to increasing with C_3H_8:O_2 ratio (see, for example 673 K). The propene selectivity, however, appears to reach a maximum for the 3% V_2O_5/TiO_2, except for the C_3H_8:O_2 ratio of 1:1 at 713 K (Fig 4.1). The propene selectivity decreases with increase in temperature. With a change in C_3H_8:O_2 ratio, no clear trend in propene selectivity is observed for a particular catalyst.

4.2.2 The effect of vanadia and chromia species on propane ODH

The effect of changing the surface metal oxide species on TiO_2 was tested by comparing the activity and selectivity trends for 1% V_2O_5/TiO_2 and 1% Cr_2O_3/TiO_2 catalysts as a function of temperature. The data from Tables 4.2 and 4.5 are used to plot Fig 4.5. The activity for both catalysts increases with temperature. This increase in activity with temperature is expected. The variation in the selectivity with increase in temperature is, however, different for the two catalysts. For 1% V_2O_5/TiO_2 the propene selectivity decreases with increase in temperature, whereas, for 1% Cr_2O_3/TiO_2 the propene selectivity increases with the temperature. Thus, surface metal oxide species has a crucial role in determining the yield of propene. Consequently, it is worthwhile to study the kinetics of the reaction to better understand the factors governing the activity and propene selectivity as a function of loading and surface metal oxide species.

4.3 Kinetic investigation

The absence of a known rate determining step and dealing with a set of rival models that appear to almost equally fit the experimental data, kinetic investigation, therefore, is a twofold problem of parameter estimation and model discrimination. Ideally, the estimated parameters, which are statistically significant, should be positive and comply with physicochemical constraints. In the present study the best model selection is based on the statistical F-test criteria for simultaneous reactions [48].

4.3.1 Parameter estimation

As discussed previously, the estimation of kinetic parameters for oxidative dehydrogenation of propane is done using genetic algorithms. Parameter estimation is based on the power law type models, whose detailed description is made in experimental section 3.4. The five catalysts considered were 1, 3 and 4% V_2O_5/TiO_2 and 1 and 4% Cr_2O_3/TiO_2.

In order to study the effect of loading for V_2O_5/TiO_2 catalyst, parameter estimation for various power law models is done using the data from Tables 4.2 to 4.4 for the 1, 3 and 4% V_2O_5/TiO_2 catalysts, respectively. Kinetic parameter estimation is based on the minimization of multiresponse objective function for simultaneous reactions. For parameter estimation, the inverse temperature is centered about the mean reaction temperature and its value is observed to be 683.16 K. This centering is applied to the concentration terms in the form of P_m. The P_m values for propane and oxygen are 0.328 and 0.141 atm, respectively. These P_m values for the propene and carbon monoxide are reported in the Tables containing the kinetic parameters. Kinetic parameter estimation is

done for all models of the present study and the parameters for each catalyst are presented in the Tables A.1 to A.4 for the four power law models.

4.3.2 Model selection

The set of simultaneous rate equations, dictated by the type of proposed model, determines the kinetic behavior of the ODH reaction scheme. When replicate experiments are not available and at the absence of pure error analysis, the criteria for selection of the best model that best explains the reaction data among the set of rival models for simultaneous reactions can be done using F-test.

Selection of a suitable model or models is dictated by the critical F^c value. The F^c values are obtained from the published data and depend on the significance level, number of parameters, number of variables and number of experimental runs. Based on the data and the model, the F_o value can be calculated. For a particular catalyst, a model is statistically significant provided, the F_o value is greater than the F^c value. Furthermore, among the F_o values obtained for different models, the one with the highest F_o value is the most suited model to describe the experimental data. The F_o and F^c values are given in the Tables 4.7 and 4.8 for V_2O_5/TiO_2 and Cr_2O_3/TiO_2 catalysts, respectively. From the Table 4.7 it is observed that all the models are statistically inadequate to describe the experimental data for the 1% V_2O_5/TiO_2 catalyst since the F_o value is less than the $F^c_{0.10}$ (F^c value at 10% significant level). Though, none of the models is statistically adequate, the highest value of F_o is obtained for the PL-1 model. In this model carbon oxides are formed as secondary products. For the 3 and 4% V_2O_5/TiO_2 catalysts it is observed that F_o values for all the models are greater than $F^c_{0.05}$ values. In fact, the F_o values are greater

than $F^c_{0.01}$ values for both the catalysts, except for the PL-2 model of 4% V_2O_5/TiO_2 catalyst. Similar to the 1% V_2O_5/TiO_2 catalyst the experimental data obtained for the 3% V_2O_5/TiO_2 is best represented by the PL-1 model. For 4% V_2O_5/TiO_2 catalyst, however, the PL-4 model best represents the experimental data. In the PL-4 model, CO is a primary and secondary product and CO_2 is produced only from CO.

The F_o and F^c values for the Cr_2O_3/TiO_2 catalysts are presented in the Table 4.8. From the Table, it is observed that for the 1% Cr_2O_3/TiO_2 catalyst, the F_o values are greater than $F^c_{0.05}$ values, except for the PL-2 model. Similar to the sub monolayer V_2O_5/TiO_2 catalyst, the F_o value for PL-1 model is highest and, thus, best explains the experimental data. For the 4% Cr_2O_3/TiO_2 catalyst the F_o values are better than even the $F^c_{0.01}$ value. Thus, all models are statistically significant. Among the different models, the highest F_o value is obtained for the PL-3 model, which suggests that this model best represents the experimental data for the 4% Cr_2O_3/TiO_2 catalyst.

4.3.3 Modeling analysis based on proposed best models

Once the most suited models have been determined based on the highest F_o values the kinetic analysis can be done in more detail. The analysis is done with respect to the loading and effect of surface metal oxide species for the best models.

The effect of vanadia or chromia loading is first analyzed with respect to ODH reaction, r_1 and the respective parameters k_{10}, E_1, $a_1$and b_1. These values are given in the Table 4.9 for the four catalysts. The values of k_{10} are observed to increase with loading for V_2O_5/TiO_2 and Cr_2O_3/TiO_2 catalysts. Specifically, for the best models k_{10} values for the 3 and 4% V_2O_5/TiO_2 catalyst and the 1 and 4% Cr_2O_3/TiO_2 catalysts are 13.25, 14.48,

2.34 and 7.46 in the respective units. Values of k_{10} are roughly scale per amount of active metal oxide site. Furthermore, comparing the two different metal oxide species it is observed that the k_{10} values for V_2O_5/TiO_2 catalysts are greater than the Cr_2O_3/TiO_2 catalysts. Thus, the higher k_{10} values suggest that V_2O_5/TiO_2 catalysts are suited to produce propene. The ranges of activation energies are, however, in different region. For the V_2O_5/TiO_2 catalysts the activation energies are 61 and 58 kJ/mol, whereas, for the Cr_2O_3/TiO_2 catalysts the activation energies are 87 and 131 kJ/mol. From the activation energy values of V_2O_5/TiO_2 catalysts, it can be inferred that same reaction path for propane ODH exists both for sub monolayer and monolayer catalysts as there is negligible difference in the activation energy values, however, for Cr_2O_3/TiO_2 catalysts, it appears that propane ODH path for sub monolayer is different from monolayer catalyst as there is considerable difference in activation energy values (44 kJ/mol). Furthermore, propane and oxygen partial pressure dependencies, a_1 and b_1, are different for the four catalysts. The propane partial pressure dependency exists for the 3 and 4% V_2O_5/TiO_2 and 1% Cr_2O_3/TiO_2, whereas, no propane dependency exists for the 4% Cr_2O_3/TiO_2. The 4% V_2O_5/TiO_2 and 4% Cr_2O_3/TiO_2 are strongly oxygen dependent, whereas, 1% Cr_2O_3/TiO_2 and 3% V_2O_5/TiO_2 are weakly oxygen partial pressure dependent.

The information about the degradation of propene can be, at the first approximation, related to the values k_{20}, the pre-exponential factor for CO formation. For the best models values of k_{20}, E_2, a_2 and b_2 are reported in the Table 4.10. For the best models, the values of k_{20} are 9.54, 7.02, 1.76 and 15.14 for 3 and 4% V_2O_5/TiO_2 and 1 and 4% Cr_2O_3/TiO_2 catalysts. The pre-exponential factors for the propene degradation are 1/3 of these values since three moles of CO are produced from the each C_3H_8. Thus, the

difference between the k_{10} and k_{20}/β is greater for the V_2O_5/TiO_2 catalysts compared to the Cr_2O_3/TiO_2 catalysts. Consequently, the net formation of propene on V_2O_5/TiO_2 catalyst is larger compared to the Cr_2O_3/TiO_2 catalysts. The activation energies for the propane degradation reaction, r_2, range from 50 to 71 kJ/mol for the four catalysts. Comparison of E_1 and E_2 values provides information regarding the temperature dependency of the related rates of propene formation and propene degradation. The difference between the E_1 and E_2 are larger for the Cr_2O_3/TiO_2 catalysts than the V_2O_5/TiO_2 catalysts. This suggests that with an increase in temperature the rate of formation of the propene would increase for the Cr_2O_3/TiO_2 catalysts, whereas, the rate of formation of propene would increase more gradually or perhaps decrease with an increase in temperature. Indeed, the propene selectivity decreases with temperature for the V_2O_5/TiO_2 catalysts and increases with temperature for the Cr_2O_3/TiO_2 catalysts as seen in Fig 4.5.

Thus, based on the kinetic parameters it is possible to explain the effect of the loading and surface metal oxide species. The values of the k_{10} and k_{20} govern the rate of propene formation and the activation energies E_1 and E_2 determine the effect of the propene selectivity with temperature. The difference in the values of E_1 between the V_2O_5/TiO_2 and Cr_2O_3/TiO_2 catalysts suggests that reaction pathways for the important ODH reaction are different.

Table 4.1: BET area values for V_2O_5/TiO_2 and Cr_2O_3/ TiO_2 catalysts

Catalyst	Surface Area (m^2/g)	Reference
TiO_2	60	Ref [28]
1% V_2O_5/TiO_2	39	Ref [28]
3% V_2O_5/TiO_2	41	Ref [28]
4% V_2O_5/TiO_2	40	Ref [36]
1% Cr_2O_3/ TiO_2	41	Ref [36]
4% Cr_2O_3/ TiO_2	n.d	

n.d not determined

Table 4.2: Input and output mole percent of components for 1% V_2O_5/TiO_2 catalyst.

Total flow rate = 50 ml/min. Weight of the catalyst = 100 mg.

Temperature (K)	Input mole (%)		Output mole (%)				C-balance C_{out}/C_{in}
	C_3H_8	O_2	C_3H_8	C_3H_6	CO_2	CO	
673	17.355	17.355	17.037	0.112	0.164	0.087	0.99
713	17.355	17.355	16.700	0.307	0.181	0.177	0.98
733	17.355	17.355	16.650	0.448	0.258	0.293	0.99
653	29.577	14.789	29.495	0.215	0.103	0.063	1.00
673	29.577	14.789	27.637	0.256	0.132	0.152	0.95
713	29.577	14.789	26.299	0.611	0.924	0.404	0.95
653	38.650	12.883	38.451	0.159	0.089	0.097	1.00
693	38.650	12.883	38.073	0.330	0.422	0.243	0.99
713	38.650	12.883	35.550	0.395	0.494	0.363	0.99
733	38.650	12.883	34.000	0.950	0.597	0.519	0.96
653	45.652	11.413	45.405	0.217	0.122	0.116	1.00
673	45.652	11.413	43.892	0.298	0.420	0.201	0.97
693	45.652	11.413	42.894	0.479	0.715	0.369	0.96

Table 4.3: Input and output mole percent of components for 3% V_2O_5/TiO_2 catalyst.

Total flow rate = 50 ml/min. Weight of the catalyst = 40 mg.

Temperature (K)	Input mole (%)		Output mole (%)				C-balance C_{out}/C_{in}
	C_3H_8	O_2	C_3H_8	C_3H_6	CO_2	CO	
653	17.355	17.355	16.620	0.297	0.132	0.135	0.98
673	17.355	17.355	16.574	0.383	0.189	0.222	0.98
693	17.355	17.355	16.399	0.476	0.335	0.361	0.99
713	17.355	17.355	15.900	0.567	0.385	0.545	0.97
673	29.577	14.789	28.768	0.501	0.165	0.195	0.99
693	29.577	14.789	28.240	0.652	0.263	0.332	0.98
713	29.577	14.789	27.501	0.836	0.499	0.522	0.97
673	38.650	12.883	37.380	0.543	0.183	0.223	0.98
693	38.650	12.883	37.353	0.729	0.306	0.381	0.99
713	38.650	12.883	36.620	0.892	0.556	0.622	0.98
633	45.652	11.413	45.051	0.483	0.135	0.176	1.00
673	45.652	11.413	44.291	0.933	0.488	0.610	1.00
693	45.652	11.413	43.290	1.098	0.771	0.955	0.98
713	45.652	11.413	43.242	1.366	1.195	1.166	0.99
733	45.652	11.413	41.877	1.628	1.172	1.520	0.97

Table 4.4: Input and output mole percent of components for 4% V_2O_5/TiO_2 catalyst.

Total flow rate = 50 ml/min. Weight of the catalyst = 30 mg.

Temperature (K)	Input mole (%)		Output mole (%)				C-balance C_{out}/C_{in}
	C_3H_8	O_2	C_3H_8	C_3H_6	CO_2	CO	
653	17.355	17.355	17.014	0.218	0.071	0.170	0.99
673	17.355	17.355	16.624	0.423	0.407	0.532	1.00
713	17.355	17.355	16.143	0.772	1.31	1.137	1.00
653	29.577	14.789	28.464	0.443	0.120	0.188	0.98
673	29.577	14.789	27.278	0.655	0.428	0.407	0.95
713	29.577	14.789	27.072	0.914	1.117	0.723	0.97
633	38.650	12.883	38.665	0.354	0.169	0.149	1.00
653	38.650	12.883	37.916	0.649	0.362	0.300	1.00
673	38.650	12.883	36.708	0.769	0.506	0.479	0.98
713	38.650	12.883	35.970	1.056	1.140	1.211	0.98
633	45.652	11.413	44.916	0.472	0.125	0.187	0.99
653	45.652	11.413	43.655	0.513	0.537	0.390	0.97
673	45.650	11.413	42.602	0.820	0.816	0.658	0.96
693	45.652	11.413	41.341	1.134	1.110	1.030	0.95

Table 4.5: Input and output mole percent of components for 1% Cr_2O_3/TiO_2 catalyst.

Total flow rate = 50 ml/min. Weight of the catalyst = 150 mg.

Temperature (K)	Input mole (%)		Output mole (%)				C-balance C_{out}/C_{in}
	C_3H_8	O_2	C_3H_8	C_3H_6	CO_2	CO	
633	17.355	17.355	16.768	0.170	0.125	0.140	1.00
653	17.355	17.355	16.103	0.250	1.732	0.232	0.98
673	17.355	17.355	15.543	0.380	2.462	0.383	0.97
673	29.577	14.789	27.994	0.171	0.741	0.130	0.96
693	29.577	14.789	27.715	0.217	0.984	0.210	0.96
713	29.577	14.789	27.313	0.299	1.220	0.378	0.95
653	38.650	12.883	38.441	0.047	0.682	0.321	1.00
673	38.650	12.883	37.731	0.245	0.813	0.356	0.98
693	38.650	12.883	37.068	0.731	1.790	0.721	1.00
713	38.650	12.883	34.741	1.100	2.290	1.039	0.96
673	45.652	11.413	45.065	0.361	1.256	0.337	1.00
653	45.652	11.413	44.605	0.496	1.368	0.527	1.00
673	45.652	11.413	44.319	0.818	1.602	0.835	0.99

Table 4.6: Input and output mole percent of components for 4% Cr_2O_3/TiO_2 catalyst.

Total flow rate = 50 ml/min. Weight of the catalyst = 50 mg.

Temperature (K)	Input mole (%)		Output mole (%)				C-balance C_{out}/C_{in}
	C_3H_8	O_2	C_3H_8	C_3H_6	CO_2	CO	
673	17.355	17.355	15.460	0.712	1.66	0.630	0.98
653	29.577	14.789	28.700	0.348	0.98	0.267	0.99
693	29.577	14.789	28.260	0.760	1.310	0.540	1.00
723	29.577	14.789	28.085	1.511	1.990	0.940	1.03
623	38.65	12.883	38.490	0.043	0.214	0.050	1.00
653	38.650	12.883	37.770	0.335	0.922	0.246	0.99
673	38.650	12.883	37.018	0.420	0.938	0.304	0.98
693	38.650	12.883	37.300	0.530	1.350	0.414	0.99
723	38.650	12.883	34.430	1.200	1.400	0.700	0.96
653	45.652	11.413	44.530	0.311	1.296	0.257	0.99
673	45.652	11.413	44.060	0.378	1.370	0.340	0.98
693	45.652	11.413	43.739	0.629	1.500	0.462	0.98

Table 4.7: Modeling (F_o) and critical (F^c) values of F-test for titania supported vanadium oxide catalysts in propane ODH reaction[5c].

Model	1% V_2O_5/TiO_2		3% V_2O_5/TiO_2			4% V_2O_5/TiO_2		
	F_o	$F^C_{0.10}$	F_o	$F^{C*}_{0.05}$	$F^C_{0.01}$	F_o	$F^C_{0.05}$	$F^C_{0.01}$
PL-1	1.56	1.675	3.74	1.917	2.496	2.57	1.930	2.520
PL-2	1.11	1.572	2.41	1.750	2.223	2.14	1.770	2.247
PL-3	1.42	1.675	3.25	1.917	2.496	2.78	1.930	2.520
PL-4	1.13	1.607	3.06	1.815	2.315	2.94	1.828	2.339

$F^{C*}_{0.05}$ = Critical value of F at 5% significant level.

Table 4.8: Modeling (F_o) and critical (F^c) values of F-test for titania supported chromium oxide catalysts in propane ODH reaction

Model	1% Cr_2O_3/TiO_2			4% Cr_2O_3/TiO_2		
	F_o	$F^C_{0.05}$	$F^C_{0.01}$	F_o	$F^C_{0.05}$	$F^C_{0.01}$
PL-1	3.05	1.944	2.547	4.168	1.960	2.579
PL-2	1.22	1.790	2.275	3.01	1.807	2.307
PL-3	2.61	1.944	2.547	4.65	1.960	2.579
PL-4	1.93	1.842	2.366	3.65	1.859	2.399

Table 4.9: Kinetic parameters from the best suited models for propane ODH reaction

V_2O_5/TiO_2			*KINETIC PARAMETER*	Cr_2O_3/TiO_2	
1%	3%	4%		1%	4%
1.59	13.25	14.48	k_{1O} *ml STP* min^{-1} *(g cat)*$^{-1}$ *atm* $^{-(a1+b1)}$	2.34	7.46
79	61	58	E_1 *kJ* mol^{-1}	87	131
0.58	0.58	0.82	a_1	0.72	0.01
0.52	0.01	0.99	b_1	0.13	0.99
PL-1	PL-1	PL-4	*Best suited model*	PL-1	PL-3

Table 4.10: Kinetic parameters from the best suited models for the degradation of propene to carbon monoxide formation

V_2O_5/TiO_2			*KINETIC PARAMETER*	Cr_2O_3/TiO_2	
1%	3%	4%		1%	4%
0.75	9.54	7.02	k_{2O} *ml STP* min^{-1} *(g cat)*$^{-1}$ *atm* $^{-(a1+b1)}$	1.76	15.14
61	50	60	E_2 *kJ* mol^{-1}	67	71
0.16	0.66	0.01	a_2	0.3	0.28
0.01	0.01	0.99	b_2	0.01	0.91
PL-1	PL-1	PL-4	*Best suited model*	PL-1	PL-3

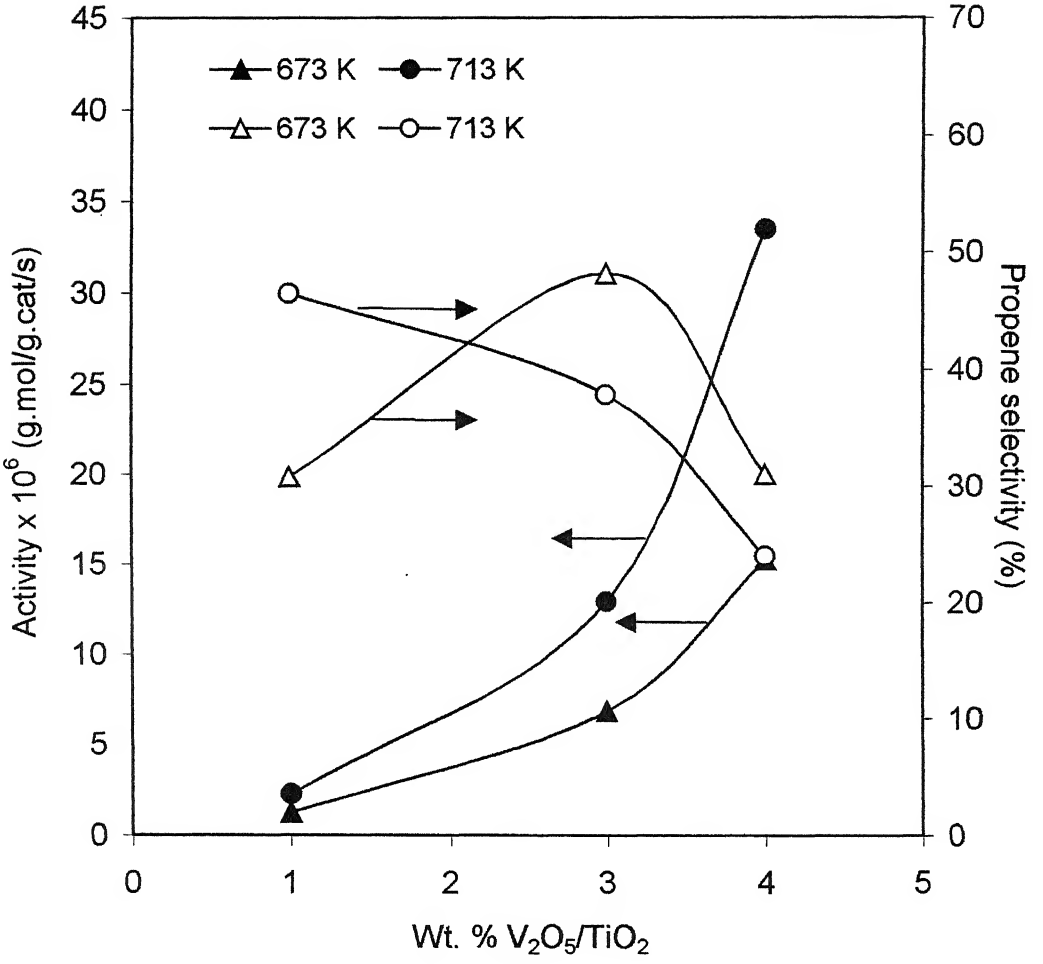

Figure 4.1: Variation of activity and propene selectivity with vanadia loading for propane ODH reaction at different temperatures. Total flow rate = 50 ml/min. Molar ratio of C_3H_8: O_2 = 1:1

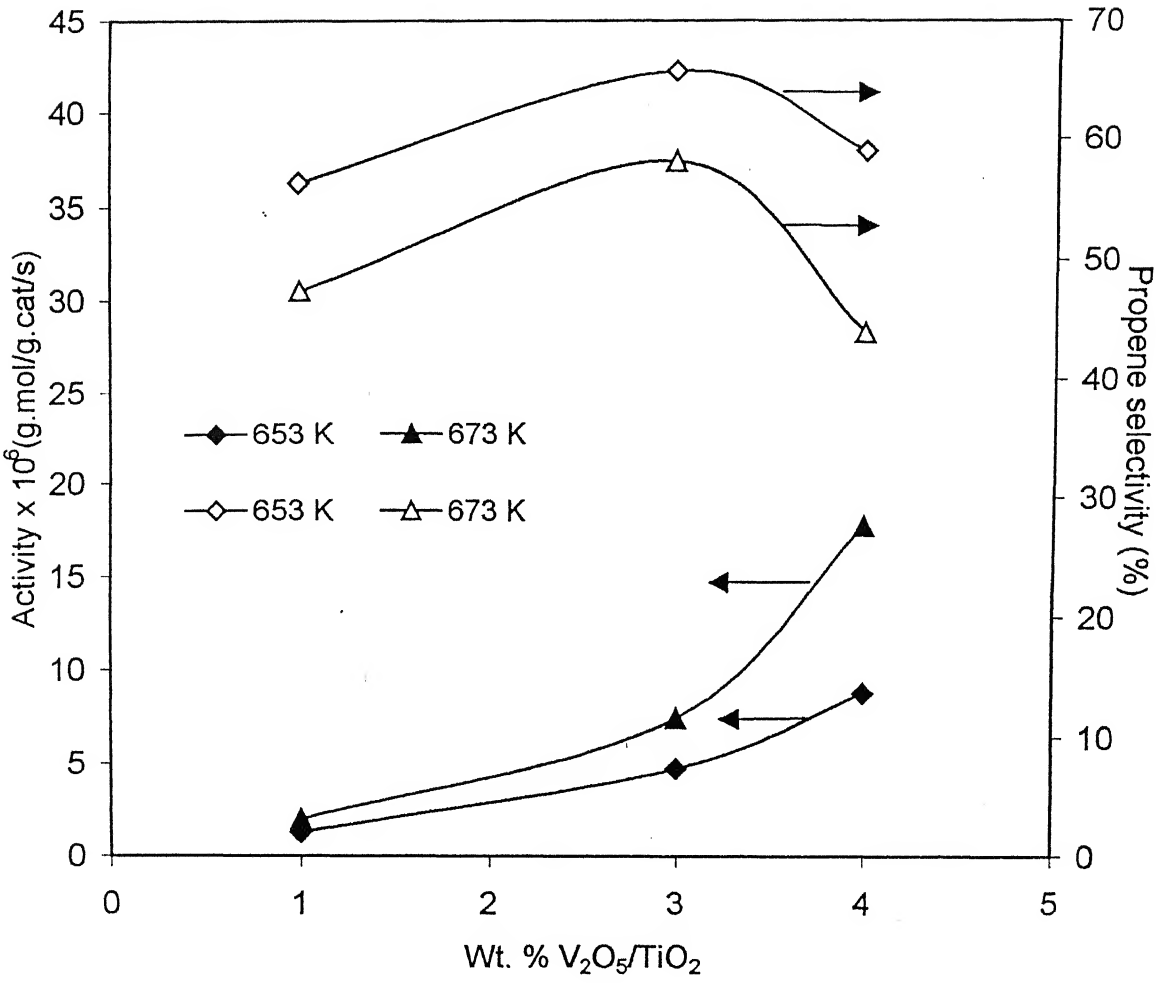

Figure 4.2: Variation of activity and propene selectivity with vanadia loading for propane ODH reaction at different temperatures. Total flow rate = 50 ml/min. Molar ratio of $C_3H_8 : O_2 = 2:1$

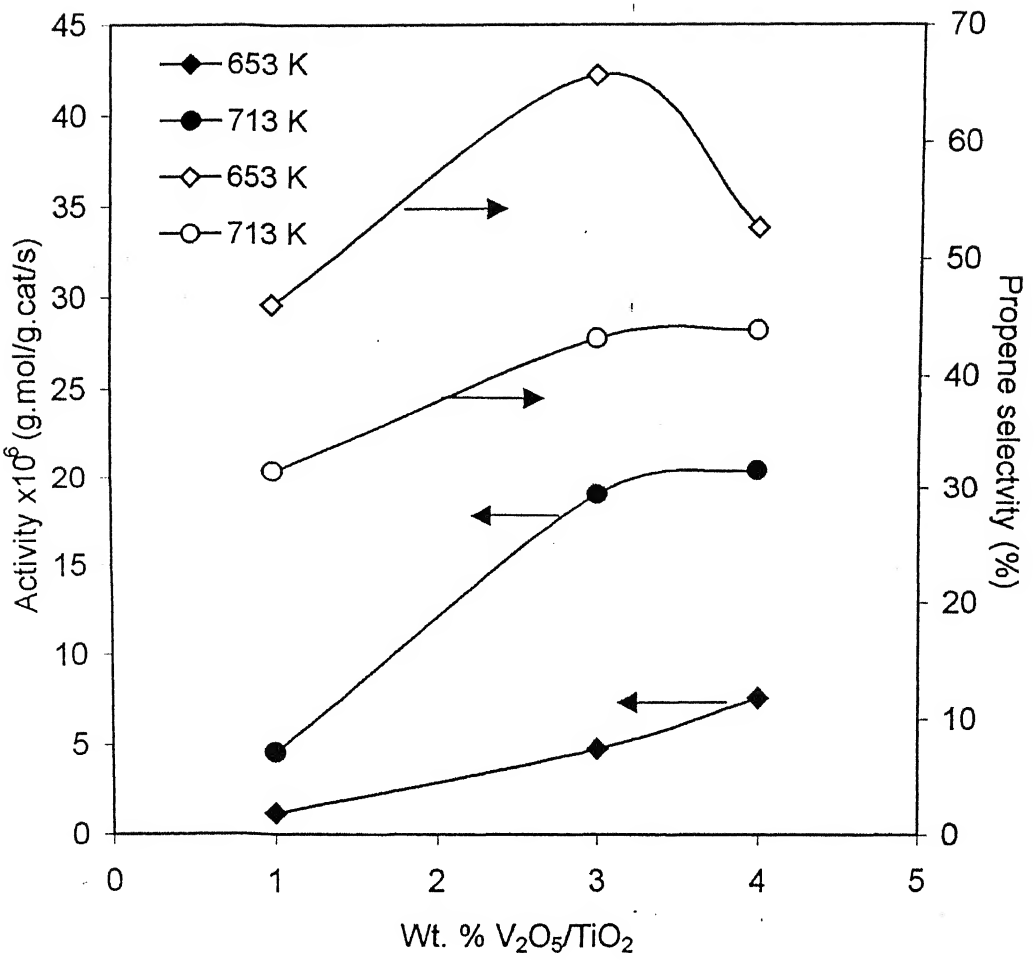

Figure 4.3: Variation of activity and propene selectivity with vanadia loading for propane ODH reaction at different temperatures. Total flow rate = 50 ml/min. Molar ratio of $C_3H_8 : O_2 = 3:1$

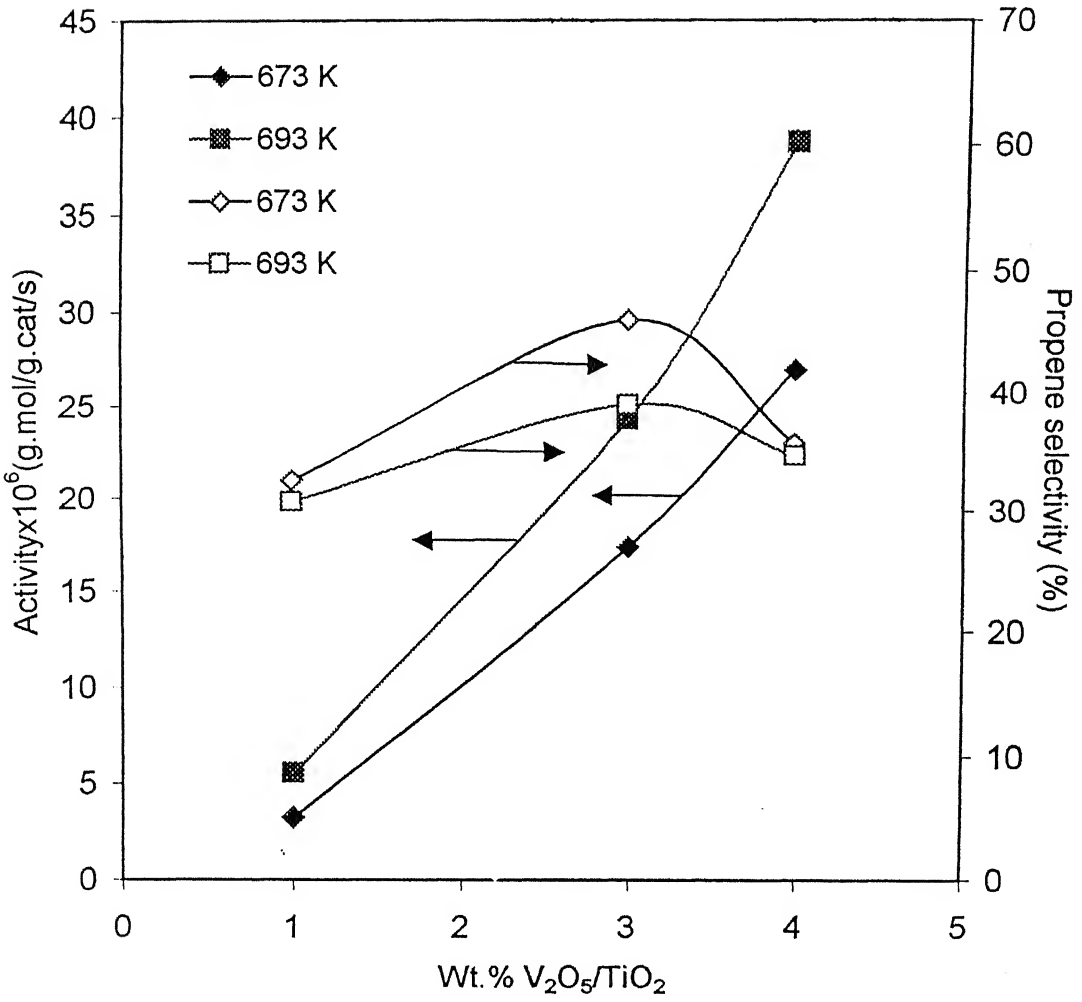

Figure 4.4: Variation of activity and propene selectivity with vanadia loading for propane ODH reaction at different temperatures. Total flow rate = 50 ml/min. Molar ratio of C_3H_8 : O_2 = 4:1

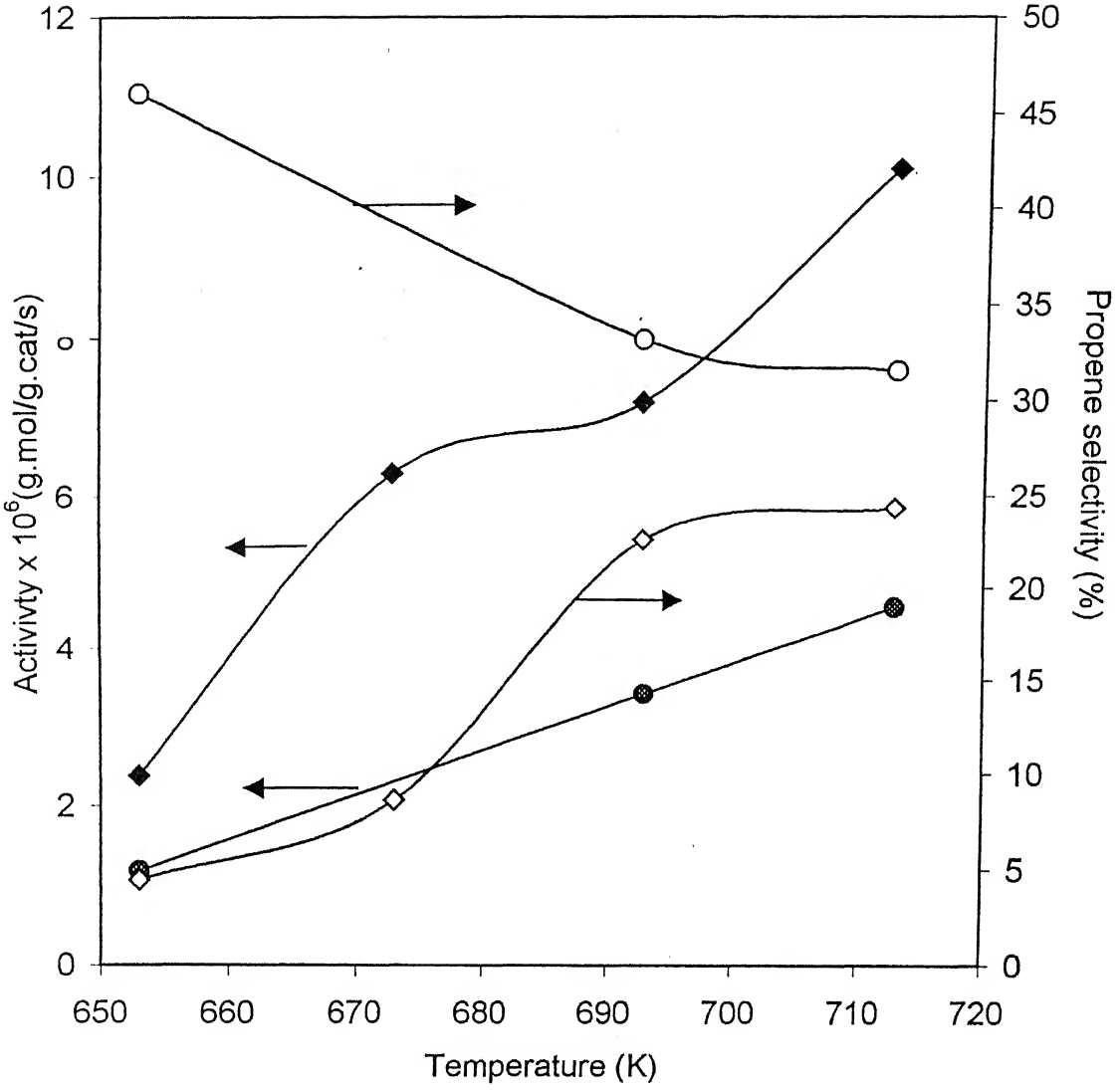

Figure 4.5: Variation of activity and propene selectivity with temperature for 1% V_2O_5/TiO_2 and 1% Cr_2O_3/TiO_2 in the propane ODH reaction. Total flow rate = 50 ml/min. Molar ratio of $C_3H_8:O_2$ = 3:1.

Legend: ○- Propene selectivity for 1% V_2O_5/TiO_2 catalyst, ●-Activity for 1% V_2O_5/TiO_2 catalyst, ◇ -Propene selectivity for 1% Cr_2O_3/TiO_2 catalyst, ◆-Activity for 1% Cr_2O_3/TiO_2 catalyst.

Chapter 5

CONCLUSIONS AND RECOMMENDATIONS

Estimation of kinetic parameters using GA in order to explain the effect of surface metal oxide species (vanadium oxide and chromium oxide) on titania support gave the insight about the propane ODH reaction kinetics.

5.1 Conclusions

Based on the reaction and modeling studies in the present study, the following conclusions can be drawn.

1. From the reaction studies, it is observed that propane conversion increase with loading for V_2O_5/TiO_2 and Cr_2O_3/TiO_2 in the region considered. This can be attributed to increase in number of two-dimensional active species, which are favorable to ODH of propane to propene. The effect of temperature, however, is different. For Cr_2O_3/TiO_2 catalysts propene selectivity increases with temperaure and for V_2O_5/TiO_2 catalysts propene selectivity decreases with temperature.
2. Using genetic algorithm the kinetic parameters for different power law models are successfully obtained.
3. For both vanadia and chromia catalysts in the ODH of propane, it appears sub monolayer loadings follow the PL-1 model and monolayer loadings follow PL-3 or PL-4 models.
4. The best suited models suggest that monolayer V_2O_5/TiO_2 and Cr_2O_3/TiO_2 catalysts favour the oxidation of carbon monoxide to carbon dioxide
5. Considering the activation energy for ODH of propane to propene, for V_2O_5/TiO_2 catalyst, the same path for ODH reaction exists for sub monolayer and monolayer

catalysts. However, for Cr_2O_3/TiO_2 catalyst, propane ODH reaction path changes from sub monolayer (1% Cr_2O_3/TiO_2) to monolayer (4% Cr_2O_3/TiO_2) catalyst.

6. Based on the kinetic parameter values the effect of loading on the propane activity and effect f the temperature on the propene selectivity can be explained.

5.2 Recommendations

The following recommendations are proposed for further study:

1. Further work on the effect of loading and nature of the surface metal oxide species should be extended to mechanistic models, which provide more information about the kinetics.

2. Detailed information can be extracted using advanced in situ techniques to find the active sites responsible for both activity and selectivity. Correlate the activity and selectivity of these catalysts with in situ characterization techniques may give more realistic information.

3. Efficient modeling can be achieved in the ODH reaction by considering the effect of water CO, CO_2 and C_3H_6 in the inlet.

9 Delmon, B., Ruiz, P., Carrazan, S. R. G., Korili, S., Rodriguez, M. A. and Sobalik, Z., *Catalysis in Petroleum Refining and Petrochemical Industries,* (1995) 1

20 Iwasawa, Y., *Studies in Surface Science and Catalysis*, Vol. 101 (1996).

21 Elsevier Science, Buonomo, F., Sanfilippo, D. and Trifiro, F., *Handbook of Heterogeneous Catalysis*, Vol.2 (1997) 2140.

22 Wachs, I. E., Handbook of spectroscopy Eds. Lewis, I. R., Edward, H. G. M., (2001) 799.

23 Wachs, I. E. and Weckhuysen, B. M., *Appl. Catal., A: Gen,* 157 (1997) 67-90.

24 Grzybowska-Swierkkosz, B., *Appl. Catal., A: Gen,* 157 (1997) 263-310

25 Bell, A. T., Iglesia, E., Su, S. and Khodakov, A., *J. Catal.,* 177 (1998) 343-351.

26 Pietrzy, S. and Genser, F., *Chem. Engg Sci.,* 54 (1999) 4315-4325.

27 Gao, X., Miguel, A. B., and. Wachs, I. E., *J. Catal.,* 188 (1999) 325-331.

28 Reddy, K. R. S. K., M.Tech Thesis, IIT Kanpur, 2002.

29 Cortez, G. G. and Banares, M. A., *J. Catal.,* 209 (2002) 197-201.

30 Hardcastle, F. D. and Wachs, I.E., *J. Mol. Catal.,* 46 (1988) 173.

31 Vuurman, M. A., Stufkens, D. J. and Oskam, A. *J. Mol. Catal.*, 60 (1990) 83.

32 Sohn, J. R.,. Ryu, S. G. and Kim, H. W., *J. Mol. Catal., A: Chem,* 135 (1998) 99-106.

33 Sohn, J. R. and Ryu, S. G., *Langmuir,* 9 (1993) 126.

34 Wachs, I. E., Deo, G., Vuurman, M. A., Hu, H., Kim, D.S and Jehng, J-M., *J. Mol. Catal.,* 82 (1993) 443.

35 Scharf, U., Schneider, H., Baiker, A. and Wokaun, A., *J. Catal.,* 145 (1994) 464.

36 Cherian, M., Ph.D Thesis, IIT Kanpur, 2002

37 Froment, G.F., *Chem. Engg. Sci.*, 42, 1987, 1073-1087.

38 Press,H., Flannery, B.P., Teukoisky, S.A, and Witterling, W.T., 1986, *Numerical Recipes*, Chap.10, Cambridge University press, New York.

9 Michalwicz, Z., genetic algorithms + data structures=Evolution program 3rd edition, Springer Berlin, 1996.

10 Wolf. D. and Moros, S., *Chem. Engrg. Sci.*, 52 (1997) 1189-1199.

41 Elliott, L., Harris, S.D., Ingham, D.B. and Wilson, C.V., *Compt. Methods. Appl. Mech. Engrg.*, 190 (2000) 1065-1095

42 Moros, R., Kalies, H., Rex, H. G. and Schaffarczyk, S., Computers & Chem. engrg, 20 (1996) 1257.

43 Polifke, W., Geng., W., and Dobbeling, K., *Combust. Flame*, 113 (1998) 119

44 Chen, K., Khodakov, A, Yang, J., Bell, A.T., and Iglesia, E., *J. Catal.*, 181(1999) 205.

45 Deb, K., Sadhana, Parts 4&5, 24(1999) 293-315.

46 Draper, N. R., Smoth, H., *Applied Regression Analysis*, 2nd edition, 1981, 464.

47 Deb. K., *Optimistion for Engineering Design* (Algorithms and examples), 3rd edition, New Delhi, 1998.

48 Froment, G. F. and Bisschoff, K. B., *Chemical Reactor Analysis and Design*, 2nd edition, New york, 1990.

49 Wechuysen, B. M., Wachs, I. E. and Jehng, J-M., *J. Phy. Chem. B* 104 (2000) 7382-7387.

50 www. itl. nist. gov/div898/handbook/eda/section3/eda3673.htm.

APPENDIX 1

A.1 Reference factor values are obtained using following formula

For hydrocarbons, the relative FID response factor is stated as:

$$F_i = \frac{(C_{aw} \, xC_n)(H_{aw} \, xH_n)}{C_{aw}} X \; 0.7487$$

Where:

F_i = relative response factor for a hydrocarbon or hydrocarbon group type of the same carbon number.

C_{aw} = atomic weight of carbon, 12.011.

C_n = number of carbon molecules in the hydrocarbon.

H_{aw} = atomic eight of hydrogen, 1.008.

H_n = number of hydrogen molecules in the hydrocarbon.

0.7487 = corrects the response of methane to unity.

Table A.1: Kinetic parameters corresponding to PL-1 model for different catalysts

KINETIC PARAMETERS	V_2O_5/TiO_2			Cr_2O_3/TiO_2	
	1%	3%	4%	1%	4%
k_{1O}	1.59	13.25	18.87	2.34	13.17
k_{2O}	0.75	9.54	10.52	1.76	6.92
k_{3O}	1.18	10.84	10.33	5.27	15.05
E_1	79	62	66	87	77
E_2	61	50	64	67	42
E_3	24	41	86	41	25
a_1	0.58	0.58	0.51	0.72	0.01
b_1	0.52	0.01	0.29	0.13	0.99
a_2	0.16	0.66	0.45	0.30	0.41
b_2	0.01	0.01	0.01	0.01	0.99
a_3	0.35	0.88	0.41	0.14	0.19
b_3	0.99	0.26	0.46	0.97	0.03
Fitness Value	6.69E-021	2.86E-021	4.02E-20	4.34E-019	8.02E-022
P_{C3H6}	3.67E-3	7.50E-3	4.40E-3	4.30E-3	6.00E-3
Generation	1000	1000	1000	1000	1000
Mass (g)	0.1	0.04	0.03	0.15	0.05

Table A.2: Kinetic parameters corresponding to PL-2 model for different catalysts

KINETIC PARAMETERS	V_2O_5/TiO_2			Cr_2O_3/TiO_2	
	1%	3%	4%	1%	4%
k_{1O}	1.23	13.01	16.50	2.26	6.97
k_{2O}	0.10	7.33	8.61	0.50	1.30
k_{3O}	0.06	6.36	4.75	2.04	4.74
k_{4O}	0.62	2.42	0.70	1.63	2.95
k_{5O}	1.00	4.41	3.90	4.74	10.20
E_1	85	59	56	101	115
E_2	142	57	70	20	105
E_3	57	29	20	86	29
E_4	62	69	193	100	82
E_5	52	95	165	77	45
a_1	0.59	0.59	0.67	0.67	0.29
b_1	0.03	0.01	0.56	0.56	0.99
a_2	0.01	0.53	0.07	0.82	0.01
b_2	0.99	0.01	0.01	0.29	0.99
a_3	0.13	0.99	0.57	0.09	0.90
b_3	0.99	0.45	0.01	0.99	0.71
a_4	0.99	0.99	0.99	0.94	0.01
b_4	0.01	0.01	0.01	0.99	0.54
a_5	0.98	0.99	0.04	0.01	0.99
b_5	0.60	0.73	0.96	0.99	0.81
Fitness Value	1.24E-021	2.08E-021	2.46E-020	3.67E-019	8.01E-022
P_{C3H6}	3.67E-3	7.50E-3	4.40E-3	4.30E-3	6.00E-3
Generation	1000	1000	1000	1000	1000
Mass (g)	0.1	0.04	0.03	0.15	0.05

Table A.3: Kinetic parameters corresponding to PL-3 model for different catalysts

KINETIC PARAMETERS	V/TiO_2			Cr/TiO_2	
	1%	3%	4%	1%	4%
k_{1O}	1.77	9.89	17.64	2.44	7.46
k_{2O}	2.68	10.53	19.20	5.60	15.14
k_{6O}	2.01	14.75	14.52	5.92	11.97
E_1	80	34	65	100	130
E_2	36	37	81	68	71
E_6	20	20	37	42	38
a_1	0.50	0.85	0.45	0.99	0.01
b_1	0.01	0.65	0.17	0.34	0.99
a_2	0.39	0.49	0.25	0.10	0.28
b_2	0.01	0.01	0.01	0.10	0.91
a_6	0.55	0.93	0.76	0.47	0.46
b_6	0.53	0.03	0.33	0.78	0.01
Fitness Value	2.00 E-021	5.38 E-021	3.80 E-020	3.98 E-019	8.29 E-021
P_{C3H6}	3.67 E-03	7.50 E-03	4.40 E-03	4.30 E-03	6.00E-03
P_{CO}	2.37 E-03	5.30 E-03	5.40 E-03	4.20 E-03	4.40 E-03
Generation	1000	1000	1000	1000	1000
Mass (g)	0.1	0.04	0.03	0.15	0.05

Table A.4: Kinetic parameters corresponding to PL-4 model for different catalysts

KINETIC PARAMETERS	1% V_2O_5/TiO_2	3% V_2O_5/TiO_2	4% V_2O_5/TiO_2	1% Cr_2O_3/TiO_2	4% Cr_2O_3/TiO_2
k_{1O}	1.66	11.96	14.49	3.06	7.13
k_{2O}	3.36	10.77	7.02	8.62	4.15
k_{4O}	0.37	6.46	6.49	0.91	16.35
k_{6O}	2.19	11.61	9.17	4.79	15.46
E_1	66	56	58	69	106
E_2	20	49	60	34	25
E_4	20	89	176	20	67
E_6	20	20	97	56	20
a_1	0.19	0.67	0.82	0.66	0.01
b_1	0.01	0.06	0.99	0.01	0.99
a_2	0.63	0.61	0.01	0.51	0.60
b_2	0.02	0.32	0.99	0.59	0.74
a_4	0.39	0.99	0.17	0.28	0.01
b_4	0.12	0.01	0.01	0.21	0.97
a_6	0.37	0.80	0.35	0.46	0.44
b_6	0.49	0.12	0.50	0.24	0.15
Fitness Value	2.32E-021	2.58E-021	3.43E-020	4.63E-019	1.55E-021
P_{C3H6}	0.0036	0.0075	0.0044	0.0043	0.0060
P_{CO}	0.0024	0.0053	0.0054	0.0042	0.0044
Generation	1000	1000	1000	1000	1000
Mass (g)	0.1	0.04	0.03	0.15	0.05